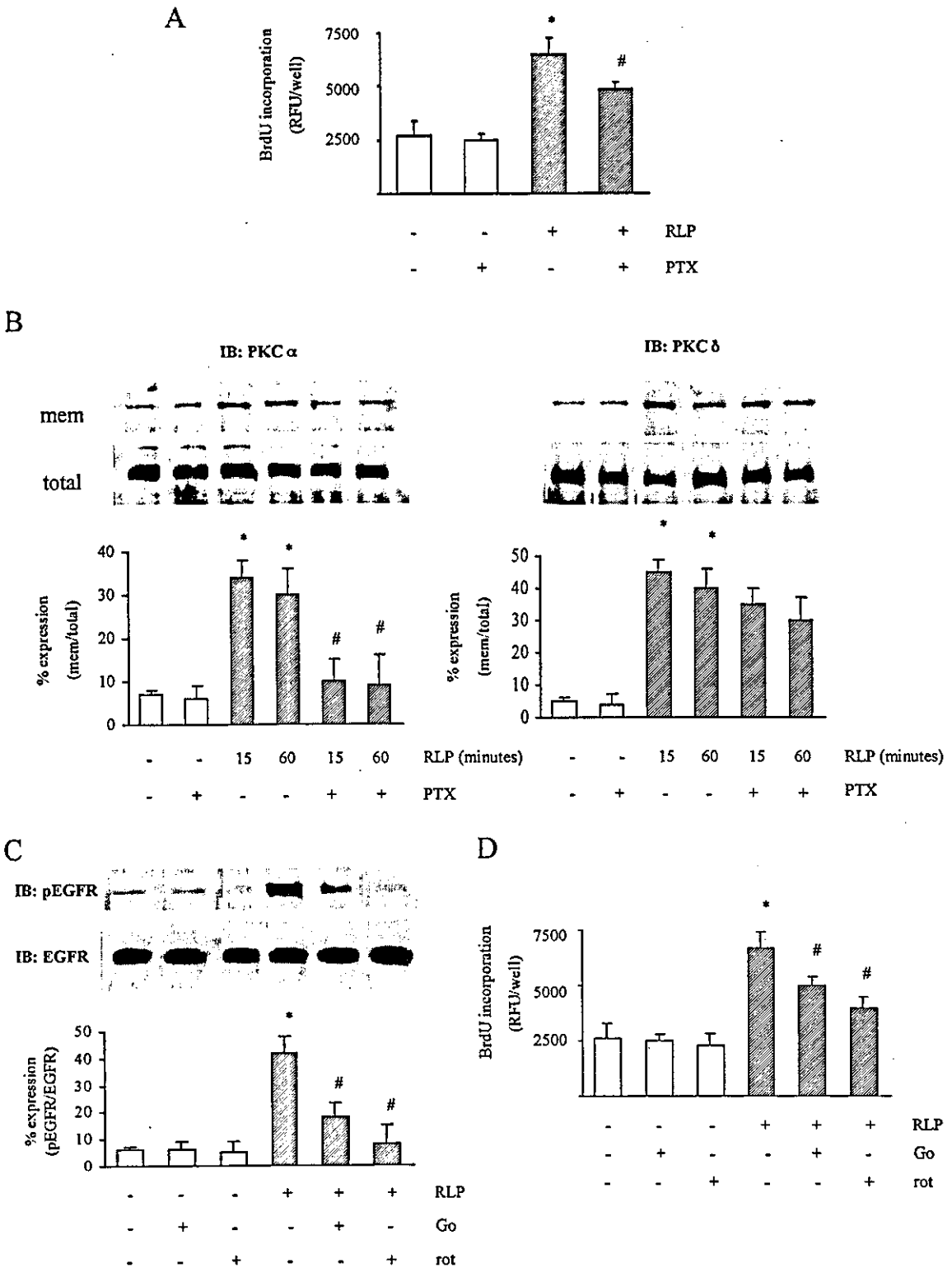

Figure 4. Involvement of G protein–coupled receptor and PKC in RLP-induced SMC proliferation. A and B, SMCs were preincubated in the absence (−) or presence (+) of pertussis toxin (PTX) (100 ng/mL) for 24 hours and then incubated in the absence (−) or presence (+) of RLPs (20 mg cholesterol per dL) for 24 hours (A) or the indicated minutes (B) before a BrdU incorporation assay (n=4) (A) or Western blotting (blots are representative of 3 separate experiments) (B). *P<0.05 vs RLP (−)/PTX (−), #P<0.05 vs RLP (+)/PTX (−). C and D, SMCs were preincubated in the absence (−) or presence (+) of Go6976 (Go) (2.5 μmol/L) or rottlerin (rot) (5 μmol/L) for 30 minutes and then incubated in the absence (−) or presence (+) of RLPs (20 mg cholesterol per dL) for 30 minutes (C) or 24 hours (D) before Western blotting (blots are representative of 3 separate experiments) (C) or a BrdU incorporation assay (n=4) (D). *P<0.01 vs RLP (−)/Go (−)/rot (−), #P<0.01 vs RLP (+)/Go (−)/rot (−).

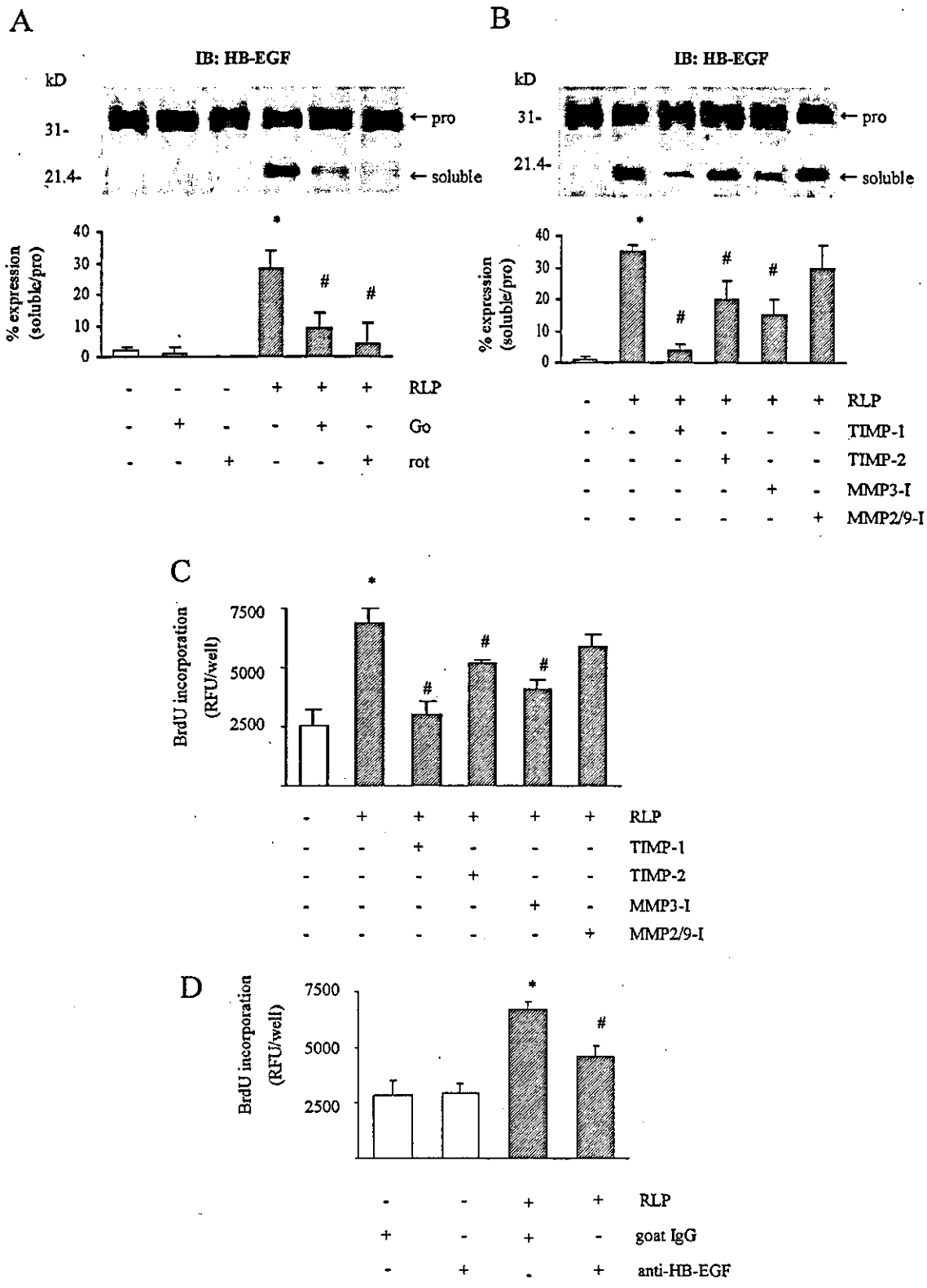

Figure 5. Involvement of HB-EGF shedding in RLP-induced SMC proliferation. A, SMCs were preincubated in the absence (−) or presence (+) of Go6976 (Go) (2.5 μmol/L) or rottlerin (rot) (5 μmol/L) for 30 minutes and then incubated in the absence (−) or presence (+) of RLPs (20 mg cholesterol per dL) for 30 minutes before Western blotting (blots are representative of 3 separate experiments). *$P<0.01$ vs RLP (−)/Go (−)/rot (−), #$P<0.01$ vs RLP (+)/Go (−)/rot (−). B and C, SMCs were preincubated in the absence (−) or presence (+) of TIMP-1 (0.5 μmol/L), TIMP-2 (0.5 μmol/L), MMP3 inhibitor (MMP3-I) (100 μmol/L), or MMP2/9 inhibitor (MMP2/9-I) (100 μmol/L) for 4 hours and then incubated in the absence (−) or presence (+) of RLPs (20 mg cholesterol per dL) for 30 minutes (B) or 24 hours (C) before Western blotting (blots are representative of 3 separate experiments) (B) or a BrdU incorporation assay (n=4) (C). *$P<0.01$ vs RLP (−)/TIMP-1 (−)/TIMP-2 (−)/MMP3-I (−)/MMP2/9-I (−), #$P<0.01$ vs RLP (+)/TIMP-1 (−)/TIMP-2 (−)/MMP3-I (−)/MMP2/9-I (−). D, SMCs were preincubated in the absence (−) or presence (+) of goat IgG (1.0 μg/mL) or anti-HB-EGF neutralizing antibody (anti-HB-EGF) (1.0 μg/mL) for 30 minutes before a BrdU incorporation assay (n=4). *$P<0.01$ vs RLP (−)/goat IgG (+)/anti-HB-EGF (−), #$P<0.01$ vs RLP (+)/goat IgG (+)/anti-HB-EGF (−).

phosphorylated as early as 15 minutes after incubation with RLPs, which preceded MAPK activation. Pretreatment with AG1478 (Calbiochem), a specific EGF receptor inhibitor, significantly inhibited RLP-induced SMC ERK activation and BrdU incorporation (Figures 3B and 3C).

Involvement of GPCR and PKC in RLP-Induced EGF Receptor Transactivation and MAPK Activation

The potential involvement of GPCR and PKC in RLP-induced SMC proliferation was then examined. Pertussis toxin (List Biological Laboratories), a G_i protein inhibitor, significantly reduced RLP-induced SMC BrdU incorporation (Figure 4A) and attenuated RLP-induced EGF receptor transactivation (data not shown). The membrane translocation of PKCα and PKCδ was increased after 15 minutes of incubation with RLPs and remained after 60 minutes (Figure 4B). Other PKC isoforms were not activated on RLP treatment (data not shown). Pretreatment of SMCs with pertussis toxin attenuated PKCα activation. In contrast, pertussis toxin treatment resulted in a partial inhibition of PKCδ activation (Figure 4B). Rottlerin (BIOMOL Research Laboratories), a specific PKCδ inhibitor, significantly reduced RLP-induced EGF receptor transactivation and SMC BrdU incorporation, as did Go6976 (Calbiochem), a specific PKCα inhibitor, though to a lesser extent (Figures 4C and 4D).

Involvement of HB-EGF Shedding in RLP-Induced EGF Receptor Transactivation

We next examined whether HB-EGF shedding is involved in RLP-induced SMC proliferation. As shown in Figures 5A and 5B, treatment with RLPs increased the amount of soluble HB-EGF in SMC membranes. In contrast, the amount of pro HB-EGF in RLP-treated SMC membranes was decreased, suggesting that the cleavage of pro-HB-EGF occurred. Interestingly, RLP did not affect total amount of HB-EGF expression. In line with the BrdU incorporation assay results, pretreatment of SMCs with rottlerin inhibited HB-EGF shedding in RLP-treated SMCs, as did Go6976, although to a lesser extent (Figure 5A). We also examined the significance of metalloproteases in this process. Matrix metalloprotease3 (MMP3) inhibitor (Calbiochem), tissue inhibitor metalloprotease-1 (TIMP-1), and, to a lesser extent, TIMP-2 (Fuji Yakuhin) reduced HB-EGF shedding in RLP-treated SMCs (Figure 5B) and attenuated RLP-induced SMC BrdU incorporation (Figure 5C). In contrast, MMP2/9 inhibitor (Calbiochem) had little effect on HB-EGF shedding and BrdU incorporation. TIMP-1 and MMP3 inhibitor also inhibited EGF receptor activation (data not shown). RLP-induced pretreatment of SMCs with anti-HB-EGF neutralizing antibody significantly reduced RLP-induced SMC BrdU incorporation (Figure 5D), indicating that HB-EGF shedding is involved, at least in part, in RLP-induced EGF receptor transactivation.

RLP-SMC Interaction and RLP-Induced SMC Proliferation

Trypsinized RLPs and RLP lipid extracts induced moderate, but statistically significant, ERK activation and SMC proliferation (Figures 6A and 6B). ApoE (Sigma), a major apolipoprotein component of RLPs, did not have an effect on SMC proliferation. Moreover, pretreatment of SMCs with heparin and heparitinase, compounds known to remove cell-surface lipoprotein lipase (LPL) and heparan-sulfate proteoglycan (HSPG), respectively, reduced PKCα and PKCδ activation (Figure 6C). When SMCs were treated with heparin or heparitinase before RLP treatment, soluble HB-EGF was decreased compared with RLP treatment alone (Figure 6D), and heparin and heparitinase also reduced RLP-induced SMC BrdU incorporation (Figure 6E).

EGF Receptor Transactivation and HB-EGF in Animal Models

To confirm the relevance of the observed RLP-induced SMC proliferation in vivo, we attempted to determine whether activation of EGF receptor and HB-EGF shedding occurred in the aortas of apoE-knockout mouse. HB-EGF shedding was detected in the apoE-knockout mice aortas but not in those of wild-type mice (Figure 7A). Moreover, an increased tyrosine phosphorylation of the EGF receptor was observed only in apoE-knockout mice (Figure 7B).

Discussion

Our present results are the first to demonstrate that proliferation of vascular SMCs triggered by RLPs involves activation of PKCs and EGF receptor transactivation. ApoE-devoid RLP (trypsinized RLP and lipid extracts from RLPs) exerted stimulatory effects on SMC proliferation, which may support the importance of RLP lipid components, as has been reported with oxidized LDL.[13] The inhibition of PKCα activation and SMC proliferation by pertussis toxin suggested that RLPs activate PKC via the GPCR signaling pathway. On the other hand, RLP-induced PKCδ activation was virtually unaffected by pertussis toxin, indicating a pertussis toxin–insensitive mechanism involved with RLP-induced SMC proliferation. In fact, both PKC and MAPK activation continued for longer than previously reported,[6] which suggests the requirements of RLP uptake and lysosomal processing for this phenomenon to occur.

We also examined the potential interaction between RLPs and SMCs. RLPs not only bind directly to cell-surface LDL receptor families but also form a complex with LPL and HSPG on the cell surface via apoE.[3,14] ApoE-devoid RLPs showed a limited effect on SMC proliferation, which may support the importance of apoE in RLP-SMC interaction. Heparin and heparitinase attenuated PKCδ and PKCα activation to a lesser extent and inhibited HB-EGF shedding, suggesting that the depletion of cell-surface LPL and HSPG decreases RLP-SMC interaction.

It has been reported that PYK2 and Src family tyrosine kinases are involved in PKC-induced EGF receptor transactivation.[15] However, PP1 and PP2, specific Src family tyrosine kinase inhibitors, had no effect on RLP-induced EGF receptor transactivation and RLPs did not affect PYK2 activity (data not shown), indicating that an alternative mechanism is involved in this process. Recently, the potential cleavage of membrane-anchored HB-EGF (pro-HB-EGF) or HB-EGF shedding by MMP/a disintegrin and metalloprotease (ADAM) families has been demonstrated in EGF

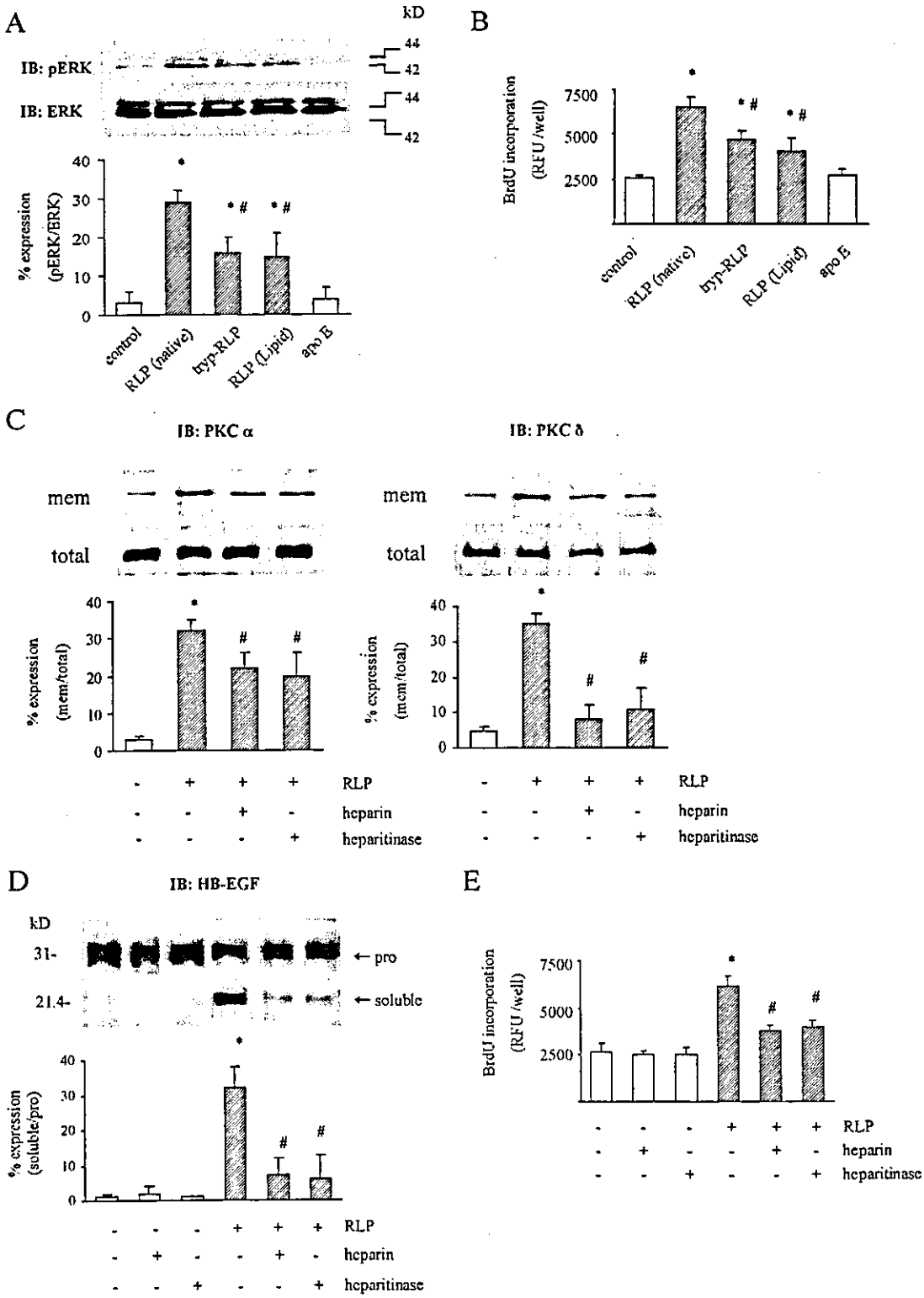

Figure 6. RLP-SMC interaction and SMC proliferation. A and B, SMCs were incubated with native RLPs (20 mg cholesterol per dL), trypsinized (tryp)-RLPs (20 mg cholesterol per dL), RLP lipid (20 mg cholesterol per dL), apoE (10 μg/mL), or medium alone (control) for 120 minutes (A) or 24 hours (B) before Western blotting (blots are representative of 3 separate experiments) (A) or a BrdU incorporation assay (n=4) (B). *$P<0.05$ vs control, #$P<0.05$ vs native RLP. C, D, and E, SMCs were preincubated in the absence (−) or presence (+) of heparin (10 μg/mL) or heparitinase (4 IU/mL) for 4 hours and then incubated with RLPs (20 mg cholesterol per dL) for 15 minutes (C), 30 minutes (D), or 24 hours (E) before Western blotting (blots are representative of 3 separate experiments) (C and D) or a BrdU incorporation assay (n=4) (E). *$P<0.01$ vs RLP (−)/heparin (−)/heparinase (−), #$P<0.01$ vs RLP (+)/heparin (−)/heparinase (−).

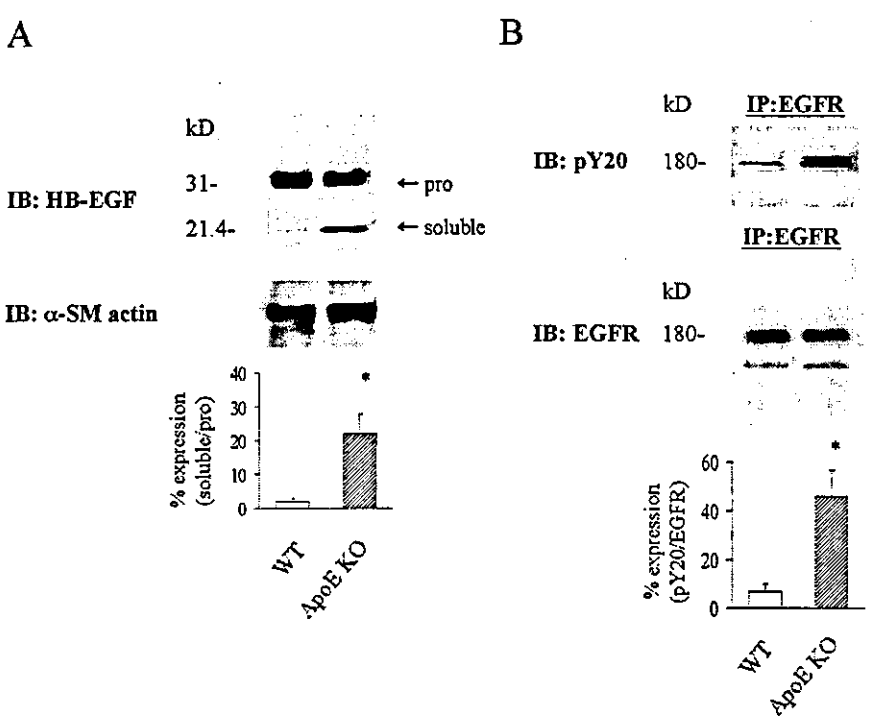

Figure 7. EGF receptor transactivation and HB-EGF shedding in animal models. A, Lysates from C57BL6 (WT) mice or apoE-knockout (apoE KO) mice aortas at 20 weeks of age were subjected to Western blotting (blots are representative of 3 separate experiments). *$P<0.05$ vs WT. B, Lysates as in panel A were immunoprecipitated with anti-EGF receptor antibody before Western blotting (blots are representative of 3 separate experiments). *$P<0.05$ vs WT.

receptor transactivation in vitro and in vivo.[16–19] Because most of the soluble HB-EGF binds to HSPG on the surface of SMCs,[20] membrane-associated soluble HB-EGF reflects the amount of HB-EGF shedding. Thus, we examined whether RLPs induce HB-EGF shedding in SMCs and successfully found detectable levels of membrane-associated soluble HB-EGF produced by RLPs, which were lowered by PKC inhibitors, suggesting that RLPs induce HB-EGF shedding via PKCs. In the present study, several MMP inhibitors attenuated RLP-induced HB-EGF shedding and EGF receptor activation. However, identification of specific MMPs responsible for this process requires additional investigation. Moreover, a remarkable difference in the inhibition of HB-EGF shedding between TIMP-1 and TIMP-2 may point to a potential involvement of ADAM families, including ADAM10, in addition to MMPs.[21] Furthermore, heparin has been shown to block the binding of soluble HB-EGF to EGF receptor.[22] Thus, heparin and heparitinase may not only decrease RLP-SMC interaction but also interfere with the binding of soluble HB-EGF generated by RLPs to EGF receptor.

We were also able to detect EGF receptor activation and HB-EGF shedding in the aortas of apoE-knockout mice, a model of spontaneous atherosclerosis exhibiting hyperremnant lipoproteinemia.[23] Although careful examinations with these animals, including involvement of PKC and MMP/ADAM families, will be required in the future to elucidate the role of RLP in vivo, these results suggest that some of the observations regarding RLP-induced SMC proliferation may be operative in vivo as well.

In the present study, anti-HB-EGF antibody and EGF receptor inhibitor failed to completely inhibit RLP-induced SMC proliferation. A PKC-dependent and EGF receptor–independent signaling pathway may be involved in this process.[24]

Taken together, we hypothesized that RLPs activate PKCs via a GPCR-dependent or -independent mechanism, followed by EGF receptor transactivation, which results in SMC proliferation. RLP-induced vascular SMC proliferation may be one of the direct causative roles of remnant lipoproteins in atherogenesis.

Acknowledgments

This work was supported by a grant from the Ministry of Education, Science, Technology and Culture of Japan (10178102) and special coordination funds from the Ministry of Education, Science, Technology and Culture of Japan. The authors gratefully acknowledge Dr Shigeki Higashiyama for providing rat recombinant HB-EGF.

References

1. McNamara JR, Shah PK, Nakajima K, et al. Remnant-like particle (RLP) cholesterol is an independent cardiovascular disease risk factor in women: results from the Framingham Heart Study. *Atherosclerosis.* 2001;154:229–236.
2. Kawakami A, Tanaka A, Nakano T, et al. Stimulation of arterial smooth muscle cell proliferation by remnant lipoprotein particles isolated by immuno-affinity chromatography with anti-apo A-I and anti-apo B-100. *Horm Metab Res.* 2001;33:67–72.
3. Kawakami A, Tanaka A, Nakano T, et al. Atorvastatin attenuates remnant lipoprotein–induced monocyte adhesion to vascular endothelium under flow conditions. *Circ Res.* 2002;91:263–271.
4. Ross R. The pathogenesis of atherosclerosis: an update. *N Engl J Med.* 1986;314:488–500.
5. Natarajan V, Scribner WM, Hart CM, et al. Oxidized low density lipoprotein-mediated activation of phospholipase D in smooth muscle cells: a possible role in cell proliferation and atherogenesis. *J Lipid Res.* 1995;36:2005–2016.
6. Zhao D, Letterman J, Schreiber BM. β-Migrating very low density lipoprotein (βVLDL) activates smooth muscle cell mitogen-activated protein (MAP) kinase via G protein-coupled receptor-mediated transactivation of the epidermal growth factor (EGF) receptor. *J Biol Chem.* 2001;276:30579–30588.
7. Argmann CA, Van Den Diepstraten CH, Sawyez CG, et al. Transforming growth factor-1 inhibits macrophage cholesteryl ester accumulation induced by native and oxidized VLDL remnants. *Arterioscler Thromb Vasc Biol.* 2001;21:2011–2018.

8. Nakajima K, Saito T, Tamura A, et al. A new assay method for the quantification of cholesterol in remnant like lipoproteins in human serum using monoclonal anti apo B-100 and apo A-I immunoaffinity mixed gels. *Clin Chim Acta.* 1993;223:53–71.
9. Bradley WA, Hwang SL, Karlin JB, et al. Low-density lipoprotein receptor binding determinants switch from apolipoprotein E to apolipoprotein B during conversion of hypertriglyceridemic very-low-density lipoprotein to low-density lipoproteins. *J Biol Chem.* 1984;259: 14728–14735.
10. Magaud JP, Sargent I, Mason DY. Detection of human white cell proliferative responses by immunoenzymatic measurement of bromodeoxyuridine uptake. *J Immunol Methods.* 1988;106:95–100.
11. Dent P, Reardon DB, Morrison DK, et al. Regulation of Raf-1 and Raf-1 mutants by Ras-dependent and Ras-independent mechanisms in vitro. *Mol Cell Biol.* 1995;15:4125–4135.
12. Okabe M, Ikawa M, Kominami K, et al. "Green mice" as a source of ubiquitous green cells. *FEBS Lett.* 1997;407:313–319.
13. Matsumura T, Sakai M, Kobori S, et al. Two intracellular signaling pathways for activation of protein kinase C are involved in oxidized low-density lipoprotein–induced macrophage growth. *Arterioscler Thromb Vasc Biol.* 1997;17:3013–3020.
14. Huff MW, Miller DB, Wolfe BM, et al. Uptake of hypertriglyceridemic very low density lipoproteins and their remnants by HepG2 cells: the role of lipoprotein lipase, hepatic triglyceride lipase, and cell surface proteoglycans. *J Lipid Res.* 1997;38:1318–1333.
15. Shah BH, Catt KJ. Calcium-independent activation of extracellularly regulated kinases 1 and 2 by angiotensin II in hepatic C9 cells: roles of protein kinase Cdelta, Src/proline-rich tyrosine kinase 2, and epidermal growth receptor trans-activation. *Mol Pharmacol.* 2002;61:343–351.
16. Suzuki M, Raab G, Moses MA, et al. Matrix metalloproteinase-3 releases active heparin-binding EGF-like growth factor by cleavage at a specific juxtamembrane site. *J Biol Chem.* 1997;272:31730–31737.
17. Izumi Y, Hirata M, Hasuwa H, et al. A metalloprotease-disintegrin, MDC9/meltrin-γ/ADAM9 and PKCδ are involved in TPA-induced ectodomain shedding of membrane-anchored heparin-binding EGF-like growth factor. *EMBO J.* 1998;17:7260–7272.
18. Prenzel N, Zwick E, Daub H, et al. EGF receptor transactivation by G-protein–coupled receptors requires metalloproteinase cleavage of proHB-EGF. *Nature.* 1999;402:884–888.
19. Asakura M, Kitakaze M, Takashima S, et al. Cardiac hypertrophy is inhibited by antagonism of ADAM12 processing of HB-EGF: metalloproteinase inhibitors as a new therapy. *Nature Med.* 2002;8:35–40.
20. Eguchi S, Dempsey PJ, Frank GD, et al. Activation of MAPKs by angiotensin II in vascular smooth muscle cells. *J Biol Chem.* 2001;276: 7957–7962.
21. Amour A, Knight CG, Webster A, et al. The in vitro activity of ADAM-10 is inhibited by TIMP-1 and TIMP-3. *FEBS Lett.* 2000;473: 275–279.
22. Kalmes A, Vesti BR, Daum G, et al. Heparin blockade of thrombin-induced smooth muscle cell migration involves inhibition of epidermal growth factor (EGF) receptor transactivation by heparin-binding EGF-like growth factor. *Circ Res.* 2000;87:92–98.
23. Plump AS, Smith JD, Hayek T, et al. Severe hypercholesterolemia and atherosclerosis in apolipoprotein E–deficient mice created by homologous recombination in ES cells. *Cell.* 1992;71:343–353.
24. Eguchi S, Iwasaki H, Inagami T, et al. Involvement of PYK2 in angiotensin II signaling of vascular smooth muscle cells. *Hypertension.* 1999; 33:201–206.

Bone Marrow Monocyte Lineage Cells Adhere on Injured Endothelium in a Monocyte Chemoattractant Protein-1–Dependent Manner and Accelerate Reendothelialization as Endothelial Progenitor Cells

Soichiro Fujiyama, Katsuya Amano, Kazutaka Uehira, Masayuki Yoshida, Yasunobu Nishiwaki, Yoshihisa Nozawa, Denan Jin, Shinji Takai, Mizuo Miyazaki, Kensuke Egashira, Takayuki Imada, Toshiji Iwasaka, Hiroaki Matsubara

Abstract—Peripheral blood (PB)-derived $CD14^+$ monocytes were shown to transdifferentiate into endothelial cell (EC) lineage cells and contribute to neovascularization. We investigated whether bone marrow (BM)- or PB-derived $CD34^-/CD14^+$ cells are involved in reendothelialization after carotid balloon injury. Although neither hematopoietic nor mesenchymal stem cells were included in human BM-derived $CD34^-/CD14^+$ monocyte lineage cells (BM-MLCs), they expressed EC-specific markers (Tie2, CD31, VE-cadherin, and endoglin) to an extent identical to mature ECs. When BM-MLCs were cultured with vascular endothelial growth factors, hematopoietic markers were drastically decreased and new EC-specific markers (Flk and CD34) were induced. BM-MLCs were intra-arterially transplanted into balloon-injured arteries of athymic nude rats. When BM-MLCs were activated by monocyte chemoattractant protein-1 (MCP-1) in vivo or in vitro, they adhered onto injured endothelium, differentiated into EC-like cells by losing hematopoietic markers, and inhibited neointimal hyperplasia. Ability to prevent neointimal hyperplasia was more efficient than that of BM-derived $CD34^+$ cells. MCP-dependent adhesion was not observed in PB-derived $CD34^-/CD14^+$ monocytes. Regenerated endothelium exhibited a cobblestone appearance, blocked extravasation of dye, and induced NO-dependent vasorelaxation. Basal adhesive activities on HUVECs under laminar flow and β_1-integrin expression (basal and active forms) were significantly increased in BM-MLCs compared with PB-derived monocytes. MCP-1 markedly enhanced adhesive activity of BM-MLCs (2.8-fold) on HUVECs by activating β_1-integrin conformation. Thus, BM-MLCs can function as EC progenitors that are more potent than $CD34^+$ cells and acquire the ability to adhere on injured endothelium in a MCP-1–dependent manner, leading to reendothelialization associated with inhibition of intimal hyperplasia. This will open a novel window to MCP-1–mediated biological actions and vascular regeneration strategies by cell therapy. (*Circ Res.* 2003;93:980-989.)

Key Words: endothelium ■ angioplasty ■ endothelial progenitor cells ■ bone marrow ■ reendothelialization

Intimal thickening and smooth muscle cell (SMC) proliferation attributable to balloon catheter denudation of endothelial cells (ECs) remain major problems after vascular manipulations.[1,2] Effective regeneration of ECs via administration of vascular endothelial growth factor (VEGF) is one of the most potent inhibitors of SMC proliferation.[3–5] VEGF-mediated reendothelialization may be partly attributable to its ability to mobilize endothelial progenitor cells (EPCs)[3] or augment NO release from the endothelium.[6]

EC migration and sprouting from locally residing endothelium and recruitment of circulating EPCs play an important role in reendothelialization in vascular repair. EPCs have been identified among human leukocytes enriched for $CD34^+$ cells.[7–10] Although earlier studies reported that adult blood-derived $CD34^+VEGFR\text{-}2^+$ angioblasts differentiate into ECs,[7–10] recent accumulating findings have suggested that peripheral blood (PB)-derived mature $CD14^+$ monocytes can also transdifferentiate into EC lineage cells under angiogenic conditions[11–14] and play a role in neovascularization via leukocyte-leukocyte interaction with $CD34^+$ cells.[13]

When monocytes were induced to infiltrate the heart by overexpression of monocyte chemoattractant protein-1

Original received May 28, 2003; resubmission received August 25, 2003; revised resubmission received September 23, 2003; accepted September 24, 2003.

From the Department of Medicine II (S.F., K.A., T. Imada, T. Iwasaka) and Medicine I (K.U.), Kansai Medical University; Department of Medical Biochemistry (M.Y., Y. Nishiwaki), Tokyo Medical and Dental University; Pharmacobioregulation Research Laboratory (Y. Nozawa), Taiho Pharmaceutical Co Ltd; Department of Pharmacology (D.J., M.M.), Osaka Medical College; Department of Cardiovascular Medicine (K.E.), Kyushu University of Medicine; and Department of Cardiovascular Medicine (H.M.), Kyoto Prefectural University of Medicine, Kyoto, Japan.

Correspondence to Hiroaki Matsubara, MD, Department of Cardiovascular Medicine, Kyoto Prefectural University of Medicine, Kamigyo-ku, Kyoto, 602-8566, Japan. E-mail matsubah@koto.kpu-m.ac.jp

Circulation Research is available at http://www.circresaha.org

DOI: 10.1161/01.RES.0000099245.08637.CE

(MCP-1), the invading monocytes seemed to form erythrocyte-containing vascular-like tunnels.[15] Considering that only ~0.05% of PB leukocytes express CD34 and yet as many as 10% to 20% of ECs are blood-derived cells in the neovasculature in ischemic tisssues,[16] such monocyte-derived EC lineage cells may also partly act as angioblasts to be incorporated into neovasculature. Although we[17,18] have demonstrated that bone marrow (BM)-derived mononuclear cells differentiate into neocapillaries in ischemic limbs or myocardium, the involvement of BM monocyte–derived EC lineage cells remains undefined. Considering that the administration of granulocyte-macrophage colony–stimulating factor mobilized angioblasts from BM[19] and that statin treatment[20,21] accelerated reendothelialization after vascular injury by mobilizing BM-derived EC lineage cells, transdifferentiation of BM monocyte lineage cells (BM-MLCs) to EC-like cells may contribute to reendothelialization. We report a novel finding that MLCs in BM cells can adhere on the injured endothelium by a MCP-1–dependent mechanism to cause reendothelialization as EC progenitors more potent than BM-derived $CD34^+$ cells, leading to inhibition of intimal hyperplasia.

Materials and Methods

MCP-1 Gene Transfection and Arterial Injury

Bupivacaine was injected into two sites of thigh muscle (750 μg per site) of immunodeficient nude rats (F344/N rnu/rnu) to induce a higher transfection efficiency of MCP-1 plasmid. Human MCP-1 plasmid DNA (300 μg) encapsulated in hemagglutinating virus of Japan liposome was injected into the same sites (2 sites in each 150 μL) 3 days after bupivacaine.[22] Three days after MCP-1 gene transfer, deendothelialization injury of left common carotid artery was produced by ballooning (3 times) with 2F Fogarty catheter. Immediately after surgery, we administered a cell solution (1 mL including 10^7 of cells) from the left common carotid artery (BM-MLCs, BM-$CD34^+$ cells, PB-derived monocytes, saline infusion control; n=12 each). Rats were killed 2 weeks after injury.

Isolation of BM-MLCs

Human BM cells were obtained with informed consent when patients with peripheral artery diseases received angiogenic cell therapy,[23] and BM mononuclear cells (BM-MNCs) were isolated by Percoll gradient centrifugation (Lymphoprep, NYCOMED).[17] $CD34^-$ fraction in BM-MNCs was negatively selected three times by $CD34^+$ antibody-coated magnetic beads (Miltenyi Biotec). $CD34^+$ cells were separated using CD34 magnetic beads. The purity of enriched $CD34^+$ cells was 88±2.7% (n=5) by FACS analysis. $CD14^+$ cells in $CD34^-$ fraction were positively selected twice by $CD14^+$ antibody-coated magnetic beads (Miltenyi Biotec). The purity of $CD14^+$ cells was >99% by flow cytometry (n=10), and $CD34^+$ cells were <1%. The $CD34^-/CD14^+$ cells were labeled with green-fluorescence cell linker (PKH2-GL, Sigma).[17]

Cell Culture and Flow Cytometry

For FACS analysis, CD14-positive cells (2×10^6 cells/dish) were plated on fibronectin-coated dishes (6-cm diameter), incubated with EGM-2 medium supplemented with VEGF (20 ng/mL), and detached with 1 mmol/L EDTA 14 days after plating. The suspended cells were treated with human IgG polyclonal antibody, washed with PBS, and then incubated with the following monoclonal antibodies: IgG1-FITC and IgG1-PE (Becton Dickinson), CD11b and CD68 (CALTAG Laboratories), CD19, CD15, CD14, CD31, and CD34 (PharMingen), CD45 (Immunotech), VE-cadherin (Chemicon), FLK-1 (Sigma), endoglin (Ancell), and polyclonal anti–Flt-1 and Tie2 antibodies (Santa Cruz). Anti-rabbit polyclonal IgG-FITC, anti-mouse monoclonal IgG-PE (DAKO), and anti-biotin PE (Miltenyi Biotec) were used as secondary antibodies. For immunohistochemical analysis, samples were snap frozen, cut with a cryostat, and incubated with anti–von Willebrand factor (anti-vWF) (DAKO), anti–endothelial NO synthase (anti-eNOS) (Calbiochem), anti–VE-cadherin (Santa Cruz), anti-CD45 (PharMingen), or anti-CD11b (PharMingen) antibody.[16]

Histological Analysis

To measure the reendothelialized area, animals were perfused in vivo with Evans Blue dye (Sigma) at time points immediately before death and the remaining denuded area was planimetrically determined. For the intima to media (I/M) ratio, serial cross sections of paraffin-embedded specimens were stained with elastic trichrome stain.

Adhesion Assay Under Laminar Flow Conditions

Adhesion assay under laminar flow was previously described.[24,25] HUVECs transfected with recombinant type 5 adenovirus E-selectin were positioned in the flow chamber (shear stresses of 1 dyne/cm^2). The entire period was recorded on videotape, and captured images were transferred to a PC computer (10 randomly selected ×20 microscopic fields for each experiment). Cells were considered to be adherent after 10 seconds of stable contact with the monolayer.

Acetylcholine-Induced Vasodilation

Resting tension of isolated cervical aorta was adjusted to 0.25 g optimal for maximal contraction as previously described.[26] Contractile response to 50 mmol/L KCl was confirmed and preincubated for equilibration with or without L-NAME (10 μmol/L) for 30 minutes. Constrictive response of aorta was induced by norepinephrine (30 nmol/L), and at the maximal constriction level, acetylcholine (10 μmol/L) was added to induce relaxation. After acetylcholine-mediated relaxation, papaverine (100 μmol/L) was added to induce maximal relaxation. Acetylcholine-mediated relaxation was assessed by percent relaxation relative to papaverine-mediated relaxation (100%).

Reverse Transcription–Polymerase Chain Reaction

Total RNA was prepared using the RNeasy kit (Quiagen). Polymerase chain reaction (PCR) protocol and primer design were performed on basis of previous studies.[11,12] PCR products for vWF, VE-cadherin, eNOS, and GAPDH were 434, 226, 836, and 301 bp, respectively.

Statistical Analysis

Statistical analyses were performed with one-way ANOVA followed by pairwise contrasts using the Dunnett's test. Data (mean±SE) were considered significant when $P<0.05$.

Results

Endothelial Marker Expression in BM-MLCs

We characterized the cell population in $CD34^-/CD14^+$ BM-MLCs by analyzing the expressions of CD3 (T cell), CD19 (B cell), CD15 (granulocytes), and CD68 (macrophage). FACS analysis (Figure 1) indicated that the expressions of these cell markers are <2.4%, whereas CD11b-positive (monocytes) or CD45-positive (monocytes/lymphocytes) cells were >99%. Endothelial-lineage precursor cells derived from hematopoietic stem cells are known to be $AC133^+/FLK^+/CD34^+$ cells.[9] Inclusion of such cell population was <1% (Figure 1). Additional analysis indicated that BM-MLCs abundantly expressed various EC markers (Tie2, 99%; VE-cadherin, 45%; endoglin, 36%) (Figure 2). Mesenchymal stem cells were defined to be endoglin positive and CD45 negative.[27]

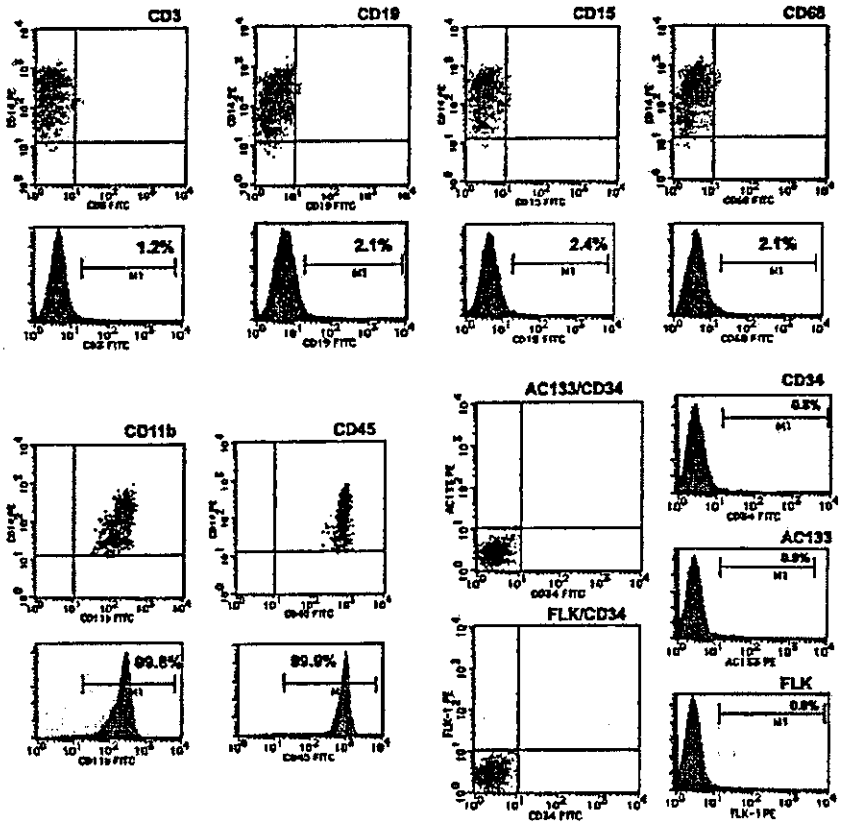

Figure 1. FACS analysis of fresh BM-MLCs. $CD34^-/CD14^+$ BM-MLCs were sorted from BM mononuclear cells and analyzed by FACS. Cells were incubated with direct-labeled monoclonal antibodies (CD14-FITC, CD3-FITC, CD19-FITC, CD15-FITC, CD68-FITC, and CD11b-FITC) or the corresponding isotype control. The quadrants were set based on IgG-FITC or IgG-PE/SSC profile. Bottom, Histogram representing cell numbers (y-axis) versus fluorescence intensity (x-axis). Similar results were obtained in 4 separate experiments. Numbers shown are the mean percent of cells for 4 separate experiments determined by comparison with the corresponding negative labeling.

Because $CD34^-/CD14^+$ BM-MLCs are CD45 positive (99.9%), it is unlikely that such mesenchymal stem cells are included in this study population. PB-derived $CD34^-/CD14^+$ cells did not express such EC markers.

When BM-MLCs were cultured for 14 days with VEGF, hematopoietic markers (CD14, CD45, and CD11b) were drastically decreased (>98% to 2.7% to 16.8%), whereas the expressions of VE-cadherin (45.3% to 88.5%), Flk (0.88% to 24.4%), endoglin (36% to 99.8%), and CD34 (0.94% to 19.3%) were increased (Figure 2A). When PB-derived $CD34^-/CD14^+$ monocytes were cultured with VEGF, marked decreases in hematopoietic markers and increase in one of EC markers (Tie2, from 11.3% to 54.7%) were observed (Figure 2B). Because other EC markers were not detected by FACS, we examined their expressions by reverse transcription (RT)-PCR. Although mRNA expressions for vWF, VE-cadherin, and eNOS were not observed in fresh day-0 PB monocytes, 28-day culture of cells with VEGF induced their mRNA expressions (Figure 2C). Thus, the present study demonstrates that characters of $CD34^-/CD14^+$ BM-MLCs are obviously different from those of PB monocytes, suggesting that our study population is mostly derived from BM-MLCs and that the influence of contaminated PB monocytes is negligible.

Time-Dependent Detachment of Balloon-Injured Endothelium

We examined time-dependent detachment of endothelium after balloon-mediated endothelial injury (Figure 3). The endothelial layer was preserved 1 day after balloon injury, as indicated by vWF expression. Detachment of endothelium was observed from day 2, and apparent intimal hyperplasia was seen on day 14 (n=12, each time point). Extravasation of Evans Blue was observed in aortic samples obtained immediately after ballooning. These findings suggest that the endothelium already lost endothelial function immediately after balloon injury, although the injured endothelial cells seemed to be present on the inner wall 1 day after balloon injury. Therefore, BM-MLCs were injected immediately after balloon injury to examine their attachment on endothelium, and reendothelialization was studied on day 14.

MCP-1–Dependent Adhesion of BM-MLCs and Reendothelialization

Planimetric analysis of rat carotid artery specimens indicated that total areas of initial balloon injury were similar between all experimental groups (no cell infusion: control, 17±1.4; BM-MLCs, 18±1.5; PB monocytes, 17±1.4 mm^2; n=12 each). Intra-arterial transfusion of BM-MLCs prelabeled with green fluorescence PKH2 showed no attachment of BM-MLCs on the injured endothelium. We hypothesized that MCP-1–activated BM-MLCs may acquire the ability to adhere on the injured endothelium by activation of β_1-integrin.[28]

We have reported that injection of naked MCP-1 plasmid into skeletal muscle causes a sustained increase (~3 fold) in the circulating MCP-1 levels over 14 days, with a peak increase at day 4.[22] Animals were pretreated with an intramuscular injection

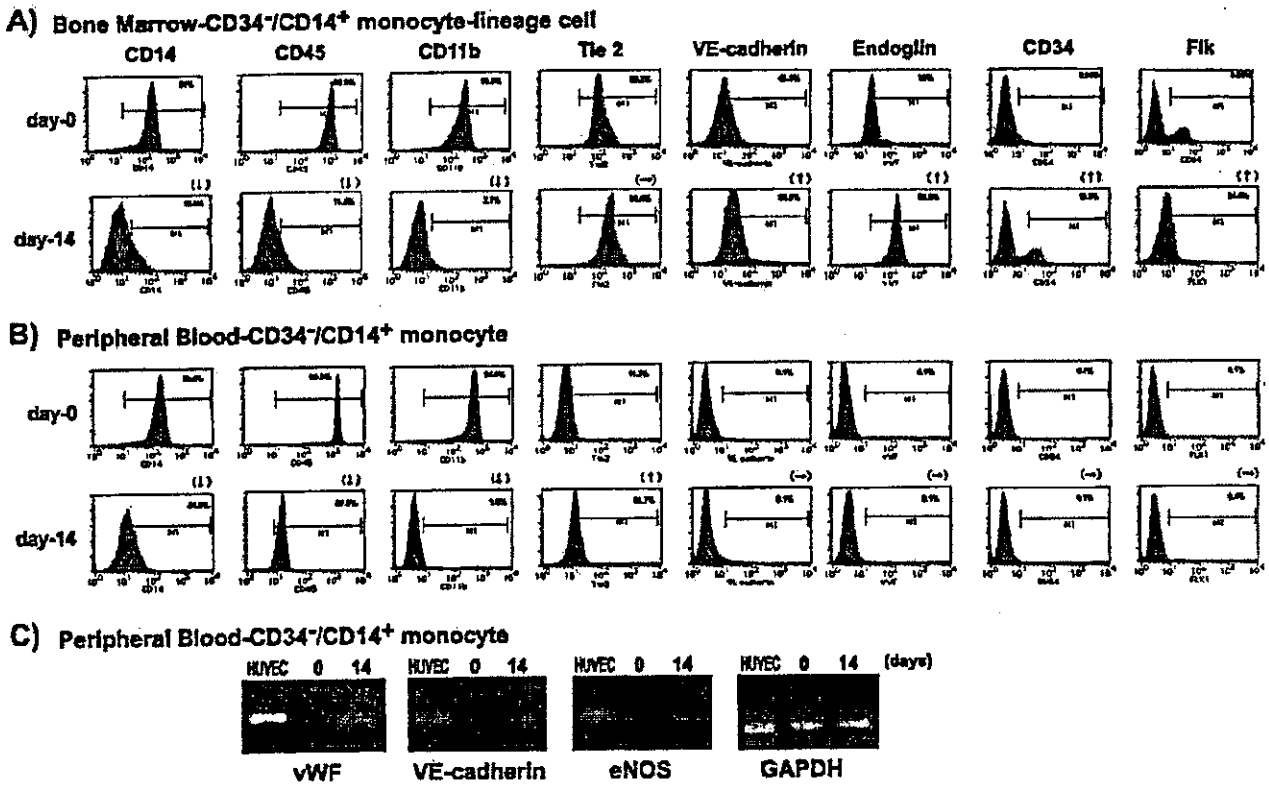

Figure 2. FACS and RT-PCR analyses of BM-MLCs after 14 days in culture with VEGF. Each panel is a histogram representing cell numbers (y-axis) versus fluorescence intensity (x-axis). BM-MLCs or PB monocytes (2×10^6cells/dish) were plated on fibronectin-coated dishes and incubated with EGM-2 medium supplemented with VEGF (20 ng/mL). The medium was exchanged every 2 days, and the cells were detached with 1 mmol/L EDTA 14 days after plating. Similar results were obtained in 4 separate experiments, and numbers shown are same as Figure 1. ↓, ↑, and → indicate the decrease, increase, and unchanged levels in the expression of surface makers, respectively. RT-PCR analysis indicates the mRNA levels for vWF, VE-cadherin, and eNOS in PB monocytes incubated with EGM-2 medium supplemented with VEGF (20 ng/mL). The expression of their mRNAs was observed 14 days after incubation but not in fresh day-0 cells. HUVEC indicates positive control.

of the MCP-1 gene, and then balloon injury and intravenous infusion of BM-MLCs were performed. BM-MLCs were transfused immediately after balloon injury, because reendothelialization efficiency was much lower when cells were infused 2 days after injury ($61\pm4\%$ versus $92\pm2.7\%$, $P<0.0001$; infusion immediately after injury; n=10 each), suggesting that the preservation of endothelial layer plays a key role for the infused BM-MLCs to attach on the inner layer.

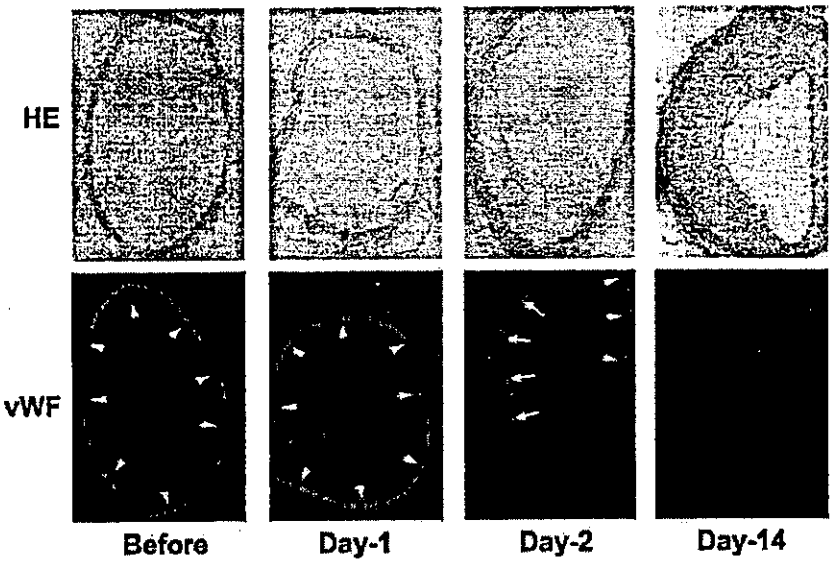

Figure 3. Endothelial detachment after balloon-mediated angioplasty. Time-dependent detachment of the endothelial layer after balloon-mediated injury was shown by H&E staining and immunofluorescence analysis. Endothelial cells were immunostained with anti-vWF antibody followed by TRITC-conjugated secondary antisera (red inner layer indicated by arrowheads). Endothelial detachment (shown by arrows) was observed at day 2, and apparent intimal hyperplasia was seen at day 14.

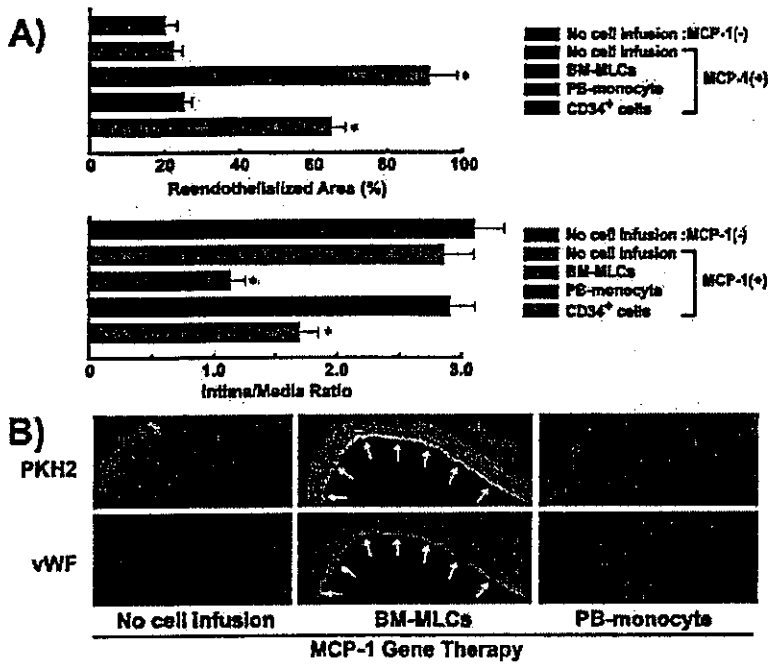

Figure 4. MCP-1–mediated adhesion of BM-MLCs and inhibition of intimal hyperplasia. A, Quantification of reendothelialized area and I/M ratio in the aortic ring expressed as mean±SE. MCP-1 plasmid was injected into the thigh muscle of rats 3 days before balloon-mediated injury. $CD34^-/CD14^+$ BM-MLCs, PB-derived $CD34^-/CD14^+$ monocytes, or BM-derived $CD34^+$ cells (10^7 cells, each) were intra-arterially transfused immediately after balloon-mediated injury. Aortic samples were examined 14 days after transfusion of cells. Reendothelialized area was evaluated by planimetric analysis (extravasation of Evans blue), and I/M ratio was determined by specimens stained by elastic trichrome stain. *$P<0.001$ vs no cell infusion (n=12 in each group). B, $CD34^-/CD14^+$ BM-MLCs or PB-derived $CD34^-/CD14^+$ monocytes (10^7 cells) were prelabeled with green fluorescence PKH2 and intra-arterially transfused immediately after injury. BM-MLCs attaching on the endothelial layer (green fluorescent indicated by white arrows) expressed endothelial marker vWF (red fluorescence indicated by white arrows) and inhibited neointimal hyperplasia 14 days after transplantation. In contrast, transfusion of PB monocyte had no effect on cell attachment or neointimal hyperplasia

MCP-1 gene treatment alone (no cell infusion) did not significantly affect vascular remodeling (reendothelialized area or I/M ratio) compared with the control (no cell infusion, without MCP-1) (Figure 4A). Transfusion of BM-derived $CD34^+$ cells (10^7 cells same as BM-MLCs number) after balloon injury of nude rats caused moderate reendothelialization (64±4%), the extent of which was relatively weaker ($P<0.001$) than that of BM-MLCs (92±2.7%), suggesting a more efficient function of BM-MLCs as an endothelial progenitor compared with $CD34^+$ fraction (Figure 4A). Reendothelialization by transplantation of $CD34^+$ cells was observed only in MCP-1–activated cells but not in MCP-1–untreated cells.

Interestingly, the green-labeled cells adhered onto the endothelial layer (Figure 4B), where reendothelialization with vWF-expressing EC-like cells was observed and intimal hyperplasia was markedly inhibited; the reendothelialized area and I/M ratio were 93±2.7% and 1.1±0.2%, respectively (n=12, Figure 4A). In contrast, infusion of PB-derived monocytes failed to cause attachment of labeled cells (Figure 4B) and showed neither reendothelialization (23±2.4%) nor inhibition of intimal hyperplasia (2.9±0.7%, n=12).

Monocytes as well as endothelium were reported to express MCP-1 receptor CCR2.[28] We next tested whether MCP-1–activated BM-MLCs or MCP-1–activated endothelium plays a more dominant role in the attachment of BM-MLCs. BM-MLCs were exposed to MCP-1 in vitro and then transfused. As shown in Figure 5A, green-labeled BM-MLCs activated by MCP-1 in vitro firmly attached onto the injured endothelium, where EC-like cells expressing eNOS (Figure 5A) as well as CD31, vWF, or VE-cadherin (not shown) accompanied the inhibition of intimal hyperplasia.

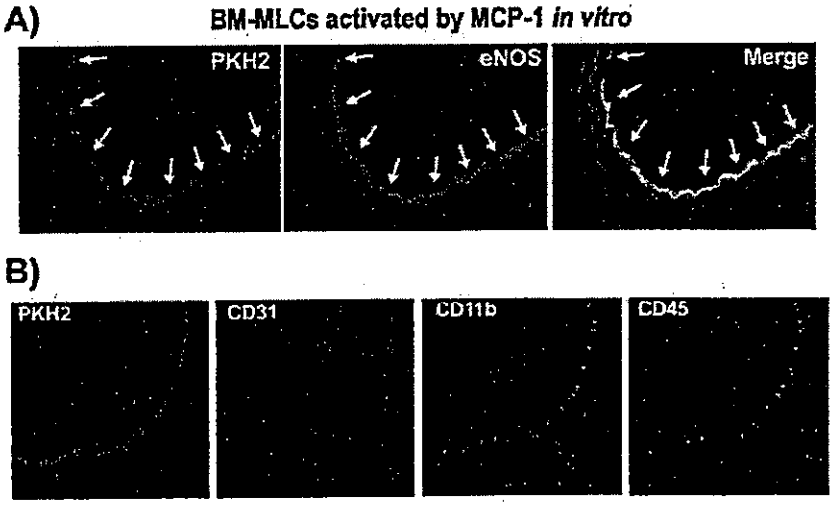

Figure 5. Adhesion and transformation of MCP-1–activated BM-MLCs to EC-like cells. BM-MLCs were incubated with serum-free medium containing MCP-1 (50 ng/mL) for 1 hour, green labeled by PKH2, and intra-arterially transfused immediately after balloon-mediated injury. A, Confocal analysis (merge with PKH2+vWF) indicated that BM-MLCs attached on the endothelial layer (green-labeled inner wall indicated by arrows) and express eNOS (red-stained inner wall indicated by arrows). B, Immunofluorescent analysis using anti-CD31 (endothelial cell marker), anti-CD11b (monocyte marker), and anti-CD45 (monocyte/lymphocyte marker) antibodies. Most of the PKH2 green-labeled BM-MLCs express CD31, whereas the numbers of BM-MLCs expressing hematopoietic markers CD11b and CD45 are very few (red-stained cells indicated by arrows).

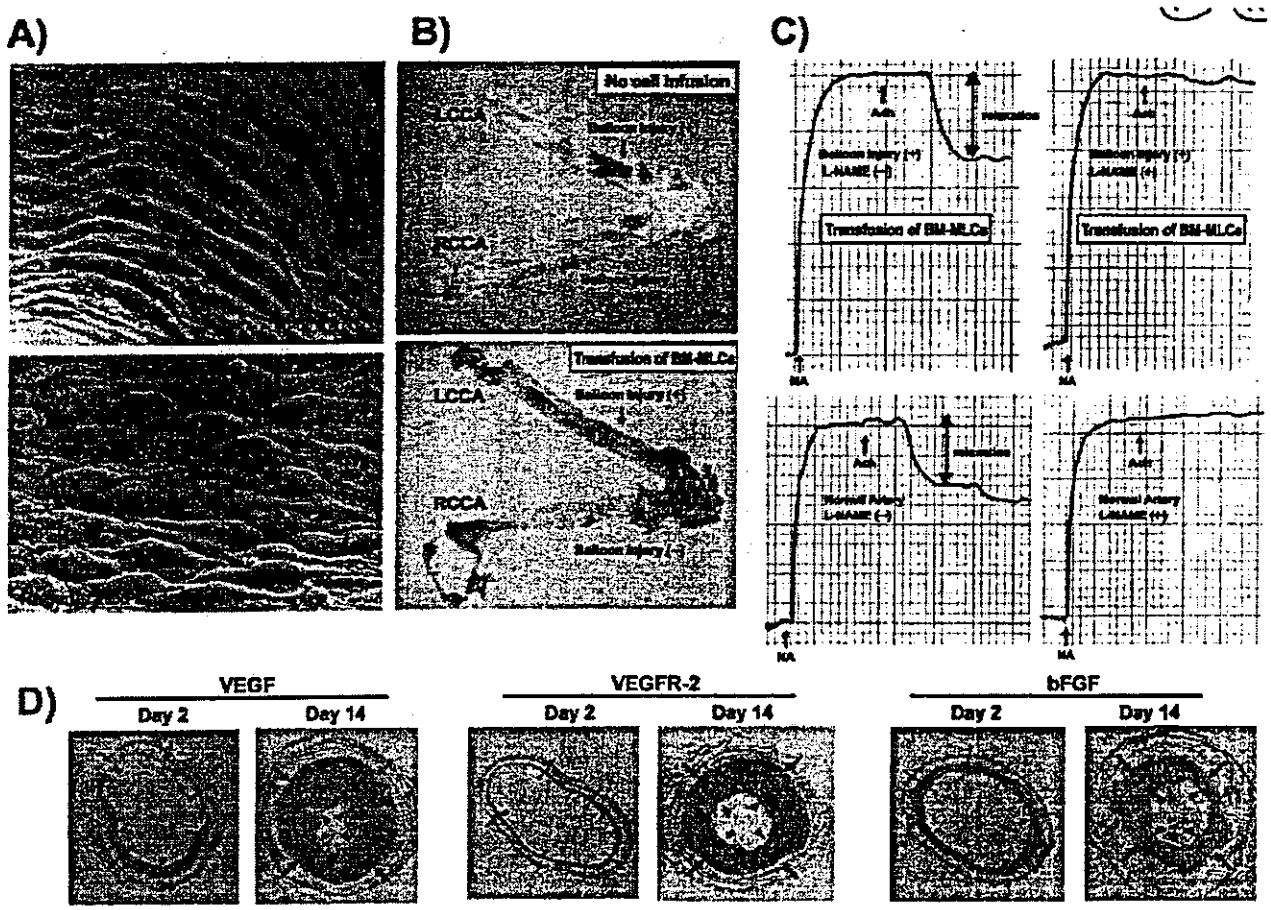

Figure 6. Electron-microscopic appearance and functional analysis of regenerated endothelium. A, Electron microscopy showing a cobblestone appearance of the regenerated endothelium by transfusion of BM-MLCs in contrast with normal endothelium covered with a monolayer coat. B, Inhibition of extravasation of Evans blue by the regenerated endothelium. LCCA indicates left common carotid artery; RCCA, right common carotid artery. C, Acetylcholine (10 μmol/L)-mediated relaxation of the carotid artery constricted by noradrenaline (30 nmol/L) with or without L-NAME treatment. D, Immunohistological analysis of aortic samples (4 and 14 days after balloon injury) using anti-VEGF, anti-VEGF receptor-2, and anti-bFGF antibodies (brown-stained neointima between arrow and arrowheads indicates immunopositive lesions). Intimal lesions abundantly express VEGF, VEGFR-2, and bFGF.

As shown in Figure 5B, EC-like cells regenerated by MCP-1–activated BM-MLCs were double-positive for PKH2 (green) and EC marker CD31 (red), whereas these transfused BM-MLCs lost the hematopoietic markers for monocytes (CD11b) or monocytes/lymphocytes (CD45), and only a few cells expressed such hematopoietic markers (indicated by arrows in Figure 5B).

Electromicroscopic and Functional Analysis

Electromicroscopic analysis revealed characteristic features of regenerated endothelium derived from BM-MLCs. The surface of the normal endothelium was smooth and covered with a monolayer coat, whereas the regenerated endothelium appeared rougher and showed a cobblestone-like appearance (Figure 6A). We next examined the function of regenerated endothelium by testing extravasation of Evans Blue. Evans Blue leaked into the medial layer in the balloon-injured endothelium, whereas there was no blue staining in the opposite normal artery with the intact endothelium (Figure 6B, top). In contrast, much less blue staining was observed in the endothelium of the balloon-injured artery treated by transfusion of BM-MLCs (Figure 6B, bottom). Quantitative analysis of BM-MLC–derived reendothelialization is shown in Figure 4A.

We additionally studied NO production from regenerated endothelium by testing acetylcholine-mediated relaxation of the carotid artery constricted by norepinephrine. Acetylcholine induced a relaxation response (40±1.9% versus papaverine-induced maximal relaxation, n=6) in the balloon-injured artery treated by transfusion of BM-MLCs, whereas L-NAME pretreatment abolished such an acetylcholine-mediated response (Figure 6C, top). This ratio of endothelial NO-dependent relaxation was comparable with that of the normal carotid artery (38±1.4%, n=6, Figure 6C, bottom).

We show in Figure 2 that hematopoietic markers on BM-MLCs were markedly decreased and in contrast EC markers were increased when BM-MLCs were cultured

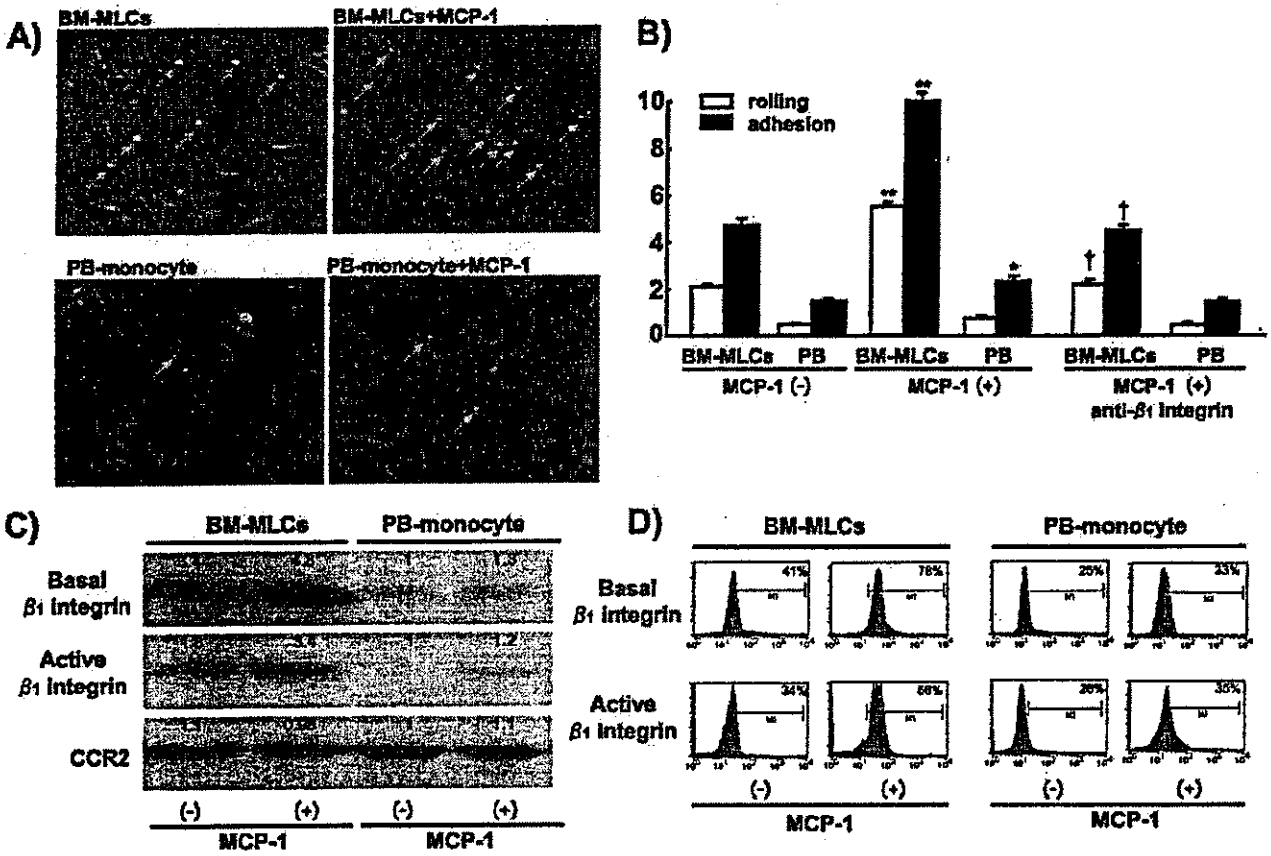

Figure 7. MCP-1–dependent adhesion of BM-MLCs and increased expressions of β_1-integrin. A, Basal rolling and adhesive activities of BM-MLCs (n=10) or PB-derived monocytes (n=8) were quantified on adeno-E-selectin transduced HUVEC monolayer under laminar flow. Adhesive and rolling cells are indicated by yellow and red arrows, respectively. Cells were considered to be adherent after 10 seconds of stable contact with the monolayer. B, Activation by MCP-1 was performed by incubating BM-MLCs or PB monocytes with MCP-1 (50 ng/mL) for 1 hour with (n=8 each) or without (n=7 each) pretreatment by anti-β_1-integrin antibody. *P<0.01, **P<0.001 vs MCP-1–untreated controls; †P<0.001 vs BM-MLCs pretreated with MCP-1 but not anti-β_1-integrin antibody. C, Cellular extracts from BM-MLCs were immunostained with antibodies specific for integrin β_1 chain (PharMingen), active conformational form of β_1-integrin (Chemicon), or CCR2 (Santa Cruz). Western blotting shows that the expressions of both basal and active forms of β_1-integrin are higher (3.4±0.3-fold and 1.8±0.2-fold, P<0.001, respectively) in BM-MLCs (n=6) relative to those in PB monocytes (n=6). MCP-1 treatment significantly (P<0.001) upregulated their expression levels in BM-MLCs (4.8±0.3-fold and 3.4±0.2-fold, respectively, P<0.001, n=8 each) but not in PB monocytes (1.3±0.2-fold and 1.2±0.2-fold, respectively, P<0.001, n=8 each). Signal densities determined by densitometry were arbitrarily calculated as values relative to the untreated PB monocytes (value=1), and the mean value is described in the Figure. D, Each panel is a histogram representing cell numbers (y-axis) versus fluorescence intensity (x-axis). Surface expression of basal or active forms of β_1-integrin was analyzed by FACS. Similar results were obtained in 4 separate experiments. Numbers shown are the mean percent of cells for 4 separate experiments determined by comparison with the corresponding negative labeling.

with VEGF. Therefore, we examined whether such VEGF system is locally activated in balloon-injured arteries. The expressions of VEGF, VEGF receptor-2, and bFGF were apparently detected in intimal lesions at day 4 after balloon injury (n=8, Figure 6D), whereas their immunostaining was not consistently observed in the earlier phase after injury (days 1 through 3, n=8, data not shown), suggesting that balloon-mediated denudation locally causes angiogenic conditions that enable EC differentiation of BM-MLCs.

MCP-1–Dependent Adhesion of BM-MLCs

We have shown in Figures 3 through 5 that BM-MLCs transfused immediately after balloon injury adhere on the endothelium in a MCP-1–dependent manner. We next investigated whether the adhesive activity of BM-MLCs on the endothelium is actually modulated by MCP-1 under flow conditions. Cellular rolling and adhesion was quantified using HUVEC monolayers perfused under laminar flow.[24,25] As shown in Figures 7A and 7B, basal rolling and adhesion activities of BM-MLCs were much higher (4.3-fold and 2.9-fold, respectively) compared with those of PB-derived $CD34^-/CD14^+$ monocytes. Interestingly, MCP-1 treatment markedly stimulated the rolling and adhesion activities of BM-MLCs (2.7-fold and 2.2-fold, respectively) relative to their basal levels, whereas MCP-1–mediated effects on PB-derived $CD34^-/CD14^+$ monocytes were much weaker.

Expression level of β_1-integrin and MCP-1–mediated activation of β_1-integrin conformation have important

implications in transendothelial chemotaxis of monocytes.[28] Neutralizing anti-β_1-integrin antibody significantly ($P<0.001$, n=8) reduced the MCP-1 effects on rolling and adhesion of BM-MLCs (Figure 7B, right). Western blotting shows that both basal expression of β_1-integrin and its active conformational change are markedly higher (3.4±0.3-fold and 1.8±0.2-fold, respectively, $P<0.001$) in BM-MLCs (n=6) relative to those in PB monocytes (n=6). MCP-1 treatment significantly ($P<0.001$) upregulated their expression levels in BM-MLCs (4.8±0.3-fold and 3.4±0.2-fold versus basal levels, respectively, $P<0.001$, n=8 each) but not in PB monocytes (1.3±0.2-fold and 1.2±0.2-fold, $P<0.001$, respectively, n=8 each). In contrast, the expression of CCR2 (MCP-1 receptor) did not differ between BM-MLCs and PB-derived monocytes (Figure 7C).

MCP-1–mediated changes in β_1-integrin expressions were additionally supported by FACS analysis (Figure 7D), which disclosed the higher expression of β_1-integrin in BM-MLCs and the more enhanced change to its active conformational form by MCP-1 compared with those in PB monocytes.

Discussion

Restenosis has remained a major clinical problem after coronary and peripheral artery angioplasty.[29] The present study demonstrates a novel strategy for vascular reendothelialization using BM-MLCs as EC progenitors and an unexpected biological action of MCP-1; BM-MLCs firmly adhered onto the injured endothelium via MCP-1–dependent β_1-integrin activation, where they transdifferentiated into functional EC-like cells and markedly inhibited intimal hyperplasia. Attached BM-MLC–derived EC-like cells have the ability to cause acetylcholine-mediated vasorelaxation in a NO-dependent manner, indicating that they have functions and characteristics similar to native ECs. Recent studies reported that PB-derived monocytes can transform into EC-like cells in the presence of VEGF.[11–14] Although the present study also showed that PB-derived monocytes have the ability to transdifferentiate into EC-like cells, the potency was much lower than BM-MLCs, and they could not adhere onto the injured endothelium even after MCP-1 stimulation.

MCP-1 binding to its receptor CCR2 induces a conformational change in β_1-integrin via $G_{i\alpha}$-mediated signaling, leading to firm adhesion on the injured endothelium.[24,28] Earlier studies have demonstrated that MCP-1 is involved in angiogenesis by promoting the migration of ECs[30] and that MCP-1 enhances capillary sprouting in ischemic limbs.[31] In the heart overexpressing MCP-1, the invading monocytes formed erythrocyte-containing vascular-like tunnels.[15] In the present study, we found that BM-MLCs require to be activated by MCP-1 in a β_1-integrin–dependent mechanism to cause a firm adhesion onto the endothelium under laminar flow. Walter et al[20] reported that statin therapy accelerates reendothelialization by increasing β_1-integrin expression on EPCs. Together, these findings suggest that the expression level of β_1-integrin and its MCP-1–mediated activation play a crucial role for the firm adhesion of BM-MLCs on injured endothelium under flow.

Elevated levels of MCP-1 were found in patients with restenosis after coronary angioplasty[32] in atherosclerotic lesions or areas of endothelial denudation.[33,34] It was reported that monocytes/macrophages migrate into the intima and media of carotid artery after balloon-mediated injury of rats and anti–MCP-1 therapy significantly prevents intimal hyperplasia.[35] Thus, migration of MCP-1–activated PB monocytes into the vessel wall is a key step in the progression of intimal hyperplasia. In this study, we focused on MCP-1–mediated action on BM-MLCs and found that this cell population has an EC-committed property. MCP-1 stimulated their adhesive activity on endothelial layer, where they preferentially transdifferentiated into endothelial-like cell rather than migration into medial layer. The MCP-1–mediated adhesive ability of BM-MLCs on the endothelium was apparently higher than that of PB monocytes. Thus, our present study demonstrates the opposite action of MCP-1 on BM-MLCs and PB monocytes; MCP-1 enhances reendothelialization by BM-MLCs associated with decreased intimal hyperplasia, whereas MCP-1 action on PB monocytes accelerates vascular remodeling. Transplantation of BM-MLCs may cause reendothelialization in vascular repair after angioplasty in situations such as atherosclerotic lesions, where systemic and local MCP-1 levels are elevated.

Blood-derived cells represented ≈10% of ECs in the neovasculature in hindlimb ischemia, and EC progenitors have been identified among leukocytes enriched for CD34-expressing cells.[7–10] Only ≈0.05% of PB leukocytes express CD34, and yet as many as 10% of ECs in the neovasculature are blood-derived cells.[8,13,15] We questioned whether such a small population of EC progenitors could have such a profound effect on neovascularization. Recent in vitro and in vivo studies reported that PB monocytes can function as EC-like cells and play a major role in new vessel formation in ischemic limbs.[11–14] In fact, we found in this study that BM-MLCs more efficiently regenerate the endothelium of injured artery compared with BM-derived $CD34^+$ cells, suggesting a more efficient function of BM-MLCs as an endothelial progenitor than $CD34^+$ fraction. It is possible that both EC progenitors and BM-MLCs mobilized from bone marrow in response to tissue ischemia are collaboratively functioning in neovascularization, to which the contribution of BM-MLCs may play a more important role.

BM-derived cells were demonstrated to differentiate into both EC-like cells and intimal smooth muscle–like cells in aortic or cardiac transplant arteriopathy.[36,37] In these allotransplant models, intimal hyperplastic lesions composed of smooth muscle–like cells and EC-like cells are barely detectable on the endothelial layer. Noishiki et al[38] established that pretreatment of vascular grafts with BM cells completely inhibited thrombus formation by reendothelialization of the inner lumen. Figure 5 showed that no transfused labeled BM-MLCs migrated into medial layer of injured artery, whereas the endothelial layer was covered with BM-MLC–derived EC-like cells. These findings suggest that if BM-MLCs preferentially transdifferentiate to endothelial-like cells on injured endothelium, infiltration of BM-derived smooth muscle–like cells into intimal lesions may be blocked

and thus restenosis can be prevented. Alternatively, precursor cells for smooth muscle–like cells may not be included in the BM-MLCs.

Our present study demonstrated that transfusion of MCP-1–activated BM-MLCs markedly prevented intimal formation by transdifferentiation into functional EC-like cells on the injured endothelium, resulting in the inhibition of growth of smooth muscle–like cells. Werner et al[39] recently reported that intravenous transfusion of spleen-derived EPC enhances reendothelialization after vascular injury when spleen is removed. MCP-1–activated BM-MLCs or spleen-derived EPCs would be available for a cell-based reendothelialization therapy. The present study will open a novel window to not only MCP-1–mediated biological actions but also more effective cell therapy strategies for vascular regeneration, because a much larger population of BM-MLCs (~10%) is present in BM cells compared with $CD34^+AC133^+FLK\text{-}1^+$ EC progenitors (~0.01%).

Acknowledgments

This study was supported in part by research grants from the Ministry of Education, Science, Sports and Culture, Japan, the Study Group of Molecular Cardiology, the Japan Medical Association, Japan Smoking Foundation, Japan Society for the Promotion of Science, Uehara Memorial Foundation, and the Japan Heart Foundation.

References

1. Libby P, Schwartz D, Brogi E, Tanaka H, Clinton SK. A cascade model for restenosis: a special case of atherosclerosis progression. *Circulation.* 1992;86:III-47–III-52.
2. Schwartz SM, De Blois D, O'Brien ERM. The intima: soil for atherosclerosis and restenosis. *Circ Res.* 1995;77:445–465.
3. Asahara T, Bauters C, Pastore C, Kearney M, Rossow S, Bunting S, Ferrara N, Symes J, Isner JM. Local delivery of vascular endothelial growth factor accelerates reendothelialization and attenuates intimal hyperplasia in balloon-injured rat carotid artery. *Circulation.* 1995;91: 2793–2801.
4. Callow AD, Choi ET, Trachtenberg JD, Stevens SL, Connolly DT, Rodi C, Ryan US. Vascular permeability factor accelerates endothelial regrowth following balloon angioplasty. *Growth Factors.* 1994;10: 223–228.
5. Laitinen M, Zachary I, Breier G, Pakkanen T, Hakkinen T, Luoma J, Abedi H, Risau W, Soma M, Laakso M, Martin JF, Yla-Herttuala S. VEGF gene transfer reduces intimal thickening via increased production of nitric oxide in carotid arteries. *Hum Gene Ther.* 1997;8:1737–1744.
6. Van der Zee R, Murohara T, Zhengyu L, Zollmann F, Passeri J, Lekutat C, Isner JM. Vascular endothelial growth factor/vascular permeability factor augments nitric oxide release from quiescent rabbit and human vascular endothelium. *Circulation.* 1997;95:1030–1037.
7. Asahara T, Murohara T, Sullivan A, Silver M, Van der Zee R, Witzenbichler B, Schatteman G, Isner JM. Isolation of putative progenitor endothelial cells for angiogenesis. *Science.* 1997;275:964–967.
8. Shi Q, Rafii S, Wu MH, Wijelath ES, Yu C, Ishida A, Fujita Y, Kothari S, Mohle R, Sauvage LA, Moore M, Storb RF, Hammond WP. Evidence for circulating bone marrow-derived endothelial cells. *Blood.* 1998;92: 362–367.
9. Peichev M, Naiyer AJ, Pereira D, Zhu Z, Lane WJ, Williams M, Oz MC, Hicklin DJ, Witte L, Moore MAS, Rafii S. Expression of VEGF-2 and AC133 by circulating human CD34+ cells identified a population of functional endothelial precursors. *Blood.* 2000;95:952–958.
10. Boyer M, Townsend LE, Vogel LM, Falk J, Reitz-Vick D, Trevor KT, Villalba M, Bendick PJ, Glover JL. Isolation of endothelial cells and their progenitor cells from human peripheral blood. *J Vasc Surg.* 2000;31: 181–189.
11. Schmeisser A, Garlichs CD, Zhang H, Eskafi S, Graffy C, Ludwig J, Strasser RH, Daniel WG. Monocytes coexpress endothelial and macrophagocytic lineage markers and form cord-like structures in matrigel under angiogenic conditions. *Cardiovasc Res.* 2001;99:671–680.
12. Pujol BF, Licibello FC, Gehling UM, Lindemann K, Weidner N, Zuzarte ML, Adamkiewicz J, Elsassere HP, Muller R, Havemann K. Endothelial-like cells derived from CD14 positive monocytes. *Differentiation.* 2000;65:287–300.
13. Harraz M, Jiao C, Hanlon HD, Hartley RS, Schatteman GC. CD34- blood-derived human endothelial progenitors. *Stem Cells.* 2001;19: 304–312.
14. Rehman J, Li J, Orschell CM, March KL. Peripheral blood "endothelial progenitor cells" are derived from monocyte/macrophages and secrete angiogenic growth factors. *Circulation.* 2003;107:1164–1169.
15. Moldovan NI, Goldschmidt-Clermount PJ, Paker-Thomburg J, Shapiro SD, Kolattukudy PE. Contribution of monocyte/macrophages to compensatory neovascularization: the drilling of metalloelastase-positive tunnels in ischemic myocardium. *Circ Res.* 2000;87:378–384.
16. Schatteman GC, Hanlon HD, Jiao C, Dodds SG, Christy BA. Blood-derived angioblasts accelerate blood-flow restoration in diabetic mice. *J Clin Invest.* 2000;106:571–578.
17. Kamihata H, Matsubara H, Fujiyama S, Masaki H, Iba O, Shintani S, Murohara T, Iwasaka T. Implantation of bone marrow mononuclear cells into ischemic myocardium enhances collateral perfusion and regional function via side supply of angioblasts, angiogenic ligands, and cytokines. *Circulation.* 2001;104:1046–1052.
18. Iba O, Matsubara H, Nozawa Y, Fujiyama S, Amano K, Mori Y, Kojima H, Iwasaka T. Angiogenesis by implantation of peripheral blood mononuclear cells and platelets into ischemic limbs. *Circulation.* 2002;106: 2019–2025.
19. Takahashi T, Kalka C, Masuda H, Chen D, Silver M, Kearney M, Magner M, Isner JM, Asahara T. Ischemia- and cytokine-induced mobilization of bone marrow-derived endothelial progenitor cells for neovascularization. *Nat Med.* 1999;5:434–438.
20. Walter DH, Rittig K, Bahlmann FH, Kirchmair R, Silver M, Murayama T, Nishimura H, Losordo DW, Asahara T, Isner JM. Statin therapy accelerates reendothelialization: a novel effect involving mobilization and incorporation of bone marrow-derived endothelial progenitor cells. *Circulation.* 2002;105:3017–3024.
21. Werner N, Priller J, Laufs U, Endres M, Bolm M, Dirnagl U, Nickenig G. Bone marrow-derived progenitor cells modulate vascular reendothelialization and neointimal formation. *Arterioscler Thromb Vasc Biol.* 2002; 22:1567–1572.
22. Egashira K, Koyanagi M, Kitamoto S, Ni W, Kataoka C, Morishita R, Kaneda Y, Akiyama C, Nishida KI, Sueishi K, Takeshita A. Anti-monocyte chemoattractant protein-1 gene therapy inhibits vascular remodeling in rats: blockade of MCP-1 activity after intramuscular transfer of a mutant gene inhibits vascular remodeling induced by chronic blockade of NO synthesis. *FASEB J.* 2000;14:1974–1978.
23. Tateishi-Yuyama E, Matsubara H, Murohara T, Ikeda U, Shintani S, Masaki H, Amano K, Shimada K, Iwasaka T, Imaizumi T. Therapeutic angiogenesis for patients with limb ischemia by autologous transplantation of bone marrow cells: a pilot study and a randomised controlled trial. *Lancet.* 2002;360:427–435.
24. Gerszten RE, Garcia-Zepeda EA, Lim YC, Yoshida M, Ding HA, Gimbrone MA, Luster AD, Luscinskas FW, Rosenzweig A. MCP-1 and IL-8 trigger firm adhesion of monocytes to vascular endothelium under flow conditions. *Nature.* 1999;398:718–723.
25. Yoshida M, Sawada T, Ishi H, Gerszten RE, Rosenzweig A, Gimbrone MA Jr, Yasukochi Y, Numano F. HMG-CoA reductase inhibitor modulates monocyte-endothelial cell interaction under physiological flow conditions in vitro. *Arterioscler Thromb Vasc Biol.* 2001;21:1165–1171.
26. Tsutusmi Y, Matsubara H, Masaki H, Kurihara H, Takai S, Miyazaki M, Nozawa Y, Ozono R, Nakagawa K, Miwa T, Kawada N, Fujiyama S, Iwasaka T. Angiotensin II type 2 receptor overexpression activates the vascular kinin system and causes vasodilation. *J Clin Invest.* 1999;104: 925–935.
27. Vogel W, Grunebach F, Messam CA, Kanz L, Brugger W, Buhring HJ. Heterogeneity among human bone marrow-derived mesenchymal stem cells and neural progenitor cells. *Haematologica.* 2003;88:126–133.
28. Springer TA. Traffic signals for lymphocyte recirculation and leukocyte emigration: the multistep paradigm. *Cell.* 1994;76:301–314.
29. Brittl JA. Advances in coronary angioplasty. *N Engl J Med.* 1996;335: 1290–1302.
30. Salcedo R, Lourdes L, Young HA, Wasserman K, Ward JM, Kleinman HK, Oppenheim JJ, Murphy WJ. Human endothelial cells express CCR2 and respond to MCP-1: direct role of MCP-1 in angiogenesis and tumor progression. *Blood.* 2000;96:34–40.

31. Ito WD, Arras M, Winkler B, Scholz D, Schaper J, Schaper W. Monocyte chemotactic protein-1 increases collateral and peripheral conductance after femoral artery occlusion. *Circ Res.* 1997;80:829–837.
32. Cipollone F, Marini M, Fazia M, Pini B, Iezzi A, Reale M, Paloscia L, Materazzo G, Erminio D, Annunzio PC, Chiarelli F, Cuccurullo F, Mezzetti A. Elevated circulating levels of monocyte chemoattractant protein-1 in patients with restenosis after coronary angioplasty. *Arterioscler Thromb Vasc Biol.* 2001;21:327–334.
33. Nelken NA, Coughlin SR, Gordon D, Wilcox JN. Monocyte chemoattractant protein-1 in human atheromatous plaques. *J Clin Invest.* 1991; 88:1121–1127.
34. Yla-Herttuala S, Lipton BA, Sarkioja T, Rosenfeld ME, Yoshimura T, Leonard EJ, Witztum JL, Steinberg D. Expression of monocyte chemoattractant protein-1 in macrophage-rich areas of human and rabbit atherosclerotic lesions. *Proc Natl Acad Sci U S A.* 1991;88:5252–5256.
35. Usui M, Egashira K, Ohtani K, Kataoka C, Ishibashi M, Hiasa K, Katoh M, Zhao Q, Kitamoto S, Takeshita A. Anti-monocyte chemoattractant protein-1 gene therapy inhibits restenotic changes (neointimal hyperplasia) after balloon injury in rats and monkeys. *FASEB J.* 2002;16: 1838–1840.
36. Shimizu K, Sugiyama S, Aikawa M, Fukumoto Y, Rabkin E, Libby P, Mitchell RN. Host bone-marrow cells are a source of donor intimal smooth-muscle-like cells in murine aortic transplant arteriopathy. *Nat Med.* 2001;7:738–741.
37. Saiura A, Sata M, Hirata Y, Nagai R, Makuuchi M. Circulating smooth muscle progenitor cells contribute to atherosclerosis. *Nat Med.* 2001;7: 382–383.
38. Noishiki Y, Tomizawa Y, Yamane Y, Matsumoto A. Autocrine angiogenic vascular prothesis with bone marrow transplantation. *Nature.* 1996;2:90–93.
39. Werner N, Junk S, Laufs U, Link A, Walenta K, Bohm M, Nickenig G. Intravenous transfusion of endothelial progenitor cells reduces neointima formation after vascular injury. *Circ Res.* 2003;93:e17–e24..

Available online at www.sciencedirect.com
SCIENCE DIRECT®
European Journal of Pharmacology 481 (2003) 217–225
ELSEVIER
ejp
www.elsevier.com/locate/ejphar

Blockade of cell adhesion by a small molecule selectin antagonist attenuates myocardial ischemia/reperfusion injury

Yasuyuki Onai[a], Jun-ichi Suzuki[a], Yasunobu Nishiwaki[a], Ryo Gotoh[a], Kurt Berens[b], Richard Dixon[b], Masayuki Yoshida[c], Hiroshi Ito[a], Mitsuaki Isobe[a,*]

[a] *Department of Cardiovascular Medicine, Tokyo Medical and Dental University, 1-5-45 Yushima, Bunkyo, Tokyo 113-8519, Japan*
[b] *Texas Biotechnology Corporation, 7000 Fannin, Suite 1920, Houston, TX 77030, USA*
[c] *Department of Medical Biochemistry, Tokyo Medical and Dental University, 1-5-45 Yushima, Bunkyo, Tokyo 113-8519, Japan*

Received 14 July 2003; received in revised form 8 September 2003; accepted 10 September 2003

Abstract

Reperfusion injury is related closely to inflammatory reactions such as the activation and accumulation of neutrophils. We investigated the efficacy of a novel small molecule selectin antagonist (bimosiamose) in a rat model of transient left coronary artery occlusion (30 min) and reperfusion (24 h). Treatment with bimosiamose (25 mg/kg, intravenously at reperfusion) showed a significant reduction in infarction area/area at risk of approximately 41% compared to vehicle control ($P = 0.01$) and preserved the left ventricular function. The accumulation of polymorphonuclear neutrophils at the site of area at risk was decreased significantly, accompanied by 78% reduction of the myeloperoxidase activity. Parallel-plate flow chamber analysis revealed that bimosiamose showed a significant inhibition in rolling (62%, $P < 0.001$) and adhesion (38%, $P < 0.05$) of HL-60 cells to activated human umbilical vein endothelial cells compared with vehicle control. This study demonstrates for the first time that bimosiamose, a novel small molecule selectin antagonist, attenuates significantly ischemia/reperfusion injury.

Keywords: Reperfusion injury; Myocardial infarction; Selectin; Cell adhesion; Echocardiography

1. Introduction

One of the most important early mechanisms of myocardial reperfusion injury is related to neutrophil attachment to the vascular endothelium with subsequent infiltration into the damaged myocardium (Hansen, 1995). Polymorphonuclear neutrophils activation causes inflammation (Entman et al., 1991), endothelial cell dysfunction (Murohara et al., 1994), and cellular necrosis (Braunwald and Kloner, 1985). The adhesion process is initiated with polymorphonuclear neutrophils rolling primarily mediated by P-selectin and E-selectin on the vascular endothelial surface and shedding of L-selectin upon neutrophil activation (Carlos and Harlan, 1994). After rolling, polymorphonuclear neutrophils adhere to endothelium more firmly and infiltrate into tissue (Hansen, 1995). Through this series of neutrophil activation, rolling and transition to firm adhesion, polymorphonuclear neutrophils accumulate in the vascular lumen and cause plugging of the microvasculature (Engler et al., 1983). Furthermore, polymorphonuclear neutrophils infiltrate into myocardium and release a variety of cell-activating and cytotoxic mediators (Neumann et al., 1997), resulting in impaired coronary reperfusion. Therefore, prevention of neutrophil accumulation is quite an effective strategy for attenuation of myocardial reperfusion injury.

Each selectin recognizes carbohydrate-containing structures. Previous studies demonstrated that sialyl Lewis^x (SLe^x), Lewis^x or Lewis^a-containing carbohydrates are major ligands of the selectin family (Foxall et al., 1992). SLe^x antagonists can be used as an inhibitor of selectin binding to their ligand. Actually, it has been reported that a monoclonal antibody against SLe^x, SLe^x analog and SLe^x-containing oligosaccharide attenuated myocardial reperfusion injury in vivo (Buerke et al., 1994; Lefer et al., 1994; Seko et al., 1996b).

* Corresponding author. Tel.: +81-3-5803-5951; fax: +81-3-5803-0238.
E-mail address: isobemi.cvm@tmd.ac.jp (M. Isobe).

0014-2999/$ - see front matter © 2003 Elsevier B.V. All rights reserved.
doi:10.1016/j.ejphar.2003.09.040

In the present study, we used a small molecule non-oligosaccharide (bimosiamose) in a well-established model of rat myocardial ischemia/reperfusion. Bimosiamose inhibits E-, P-, and L-selectin binding to their ligand, SLe^x, generally and is more potent than SLe^x in vitro study (Kogan et al., 1998). The main purpose of this study was to determine the effects of bimosiamose on myocardial reperfusion injury, physiological cardiac function, and adherence of polymorphonuclear neutrophils to the vascular endothelium under physiological flow condition.

2. Materials and methods

2.1. Surgical procedures

Eight to ten-week-old male Sprague–Dawley rats (250 to 300 g weight) were used in this experiment. Rats were anesthetized with 40 mg/kg sodium pentobarbital intraperitoneally (i.p.) immediately before operation. Rats were intubated orally with a polyethylene tube for artificial respiration (SN-480-7, Shinano, Tokyo, Japan). The left anterior descending coronary artery was visualized using a microscopy and ligated with 6–0 silk suture. Myocardial ischemia was confirmed by epicardial cyanosis and wall asynergy. After 30 min of coronary artery occlusion, reperfusion was made by loosening the suture and verified visually. The chest wall and the skin were then closed with 3–0 silk suture. Animals used in this study were maintained in accordance with the *Guide for the Care and Use of Laboratory Animals* published by the US National Institute of Health (NIH Publication No. 85-23, revised 1996).

2.2. Reagents

The structure of bimosiamose (TBC-1269) elucidates two mannoses and two carboxylic acid groups in a configuration to mimic the dimeric structure of SLe^x (Fig. 1). TBC-1900, which differs from bimosiamose in only one bond located within the 6-carbon chain joining the two biphenyl moieties, was used as an inactive control compound. Bimosiamose and TBC-1900 were kindly donated by Texas Biotechnology (Houston, TX).

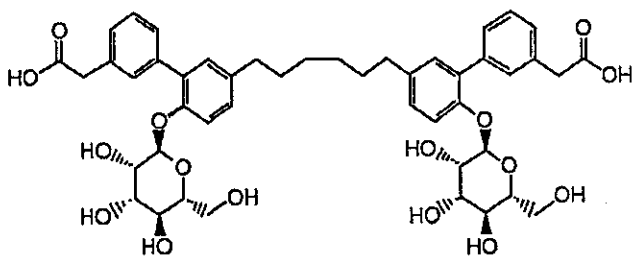

Fig. 1. Structure of bimosiamose (TBC 1269). Bimosiamose is a non-oligosaccharide glycomimetic and characterized as a small molecule (molecular weight 862.94).

2.3. Treatment protocol

The animals were assigned randomly into one of three treatment groups ($n=7$ each), as follows: (a) intravenous bimosiamose (25 mg/kg) at reperfusion; (b) intravenous TBC1900 (25 mg/kg) at reperfusion; (c) sham-operated animals (thoracotomy with left anterior descending artery isolation but without ligation).

2.4. Measurement of area at risk and infarct sizes

At the end of 24 h of reperfusion, the anesthetized rats were intubated and thracotomy was repeated. The left anterior descending artery was religated tightly and Evans blue dye (2 ml of 1.0% solution) was infused via an inferior vena cava to determine the nonischemic zone (area not at risk). Hearts were then sliced transversely into four slices, and incubated in 2.0% triphenyl tetrazolium chloride (TTC) (Sigma, Tokyo, Japan) for 15 min at 37 °C to verify the viable and necrotic area in the ischemic myocardium (area at risk) as described earlier (Vivaldi et al., 1985). Each slice was weighed and photographed, and the areas of infarction, risk, and left ventricle were evaluated using computer-assisted planimetry (Scion Image β4.0.2) by observers blinded to the treatment protocol. The volumes of each area were determined by the following process: volume of area $=(A_1 \times Wt_1)+(A_2 \times Wt_2)+(A_3 \times Wt_3)+(A_4 \times Wt_4)$ where A is the percentage of each area by planimetry from subscripted numbers 1–4 indicating sections and Wt is the weight of the same numbered sections.

2.5. Measurement of rat heart cardiac function

Rats were anesthetized mildly with sodium pentobarbital. Transthoracic echocardiography was performed with a commercially available ultrasound machine (*Nemio*, Toshiba, Tokyo, Japan) before the operation, immediately after reperfusion and 24 h after reperfusion. A 7-MHz annular array transducer was used. Hearts were imaged in the two-dimensional mode in short-axis views at the level of papillary muscle. M-mode views were used to measure the left ventricular (LV) dimensions. LV end-diastolic dimension (LVDd) and end-systolic dimension (LVDs), and fractional shortening (FS% $=[(LVDd - LVDs)/LVDd] \times 100$) were calculated from the M-mode recordings. Each dimension was presented as the average of measurements of three selected consecutive beats.

2.6. Assessment of myocardial neutrophil infiltration

To determine the extent of the polymorphonuclear neutrophil infiltration, histological staining was performed on the midventricular cardiac sections. After the myocar-

dial ischemia/reperfusion protocol, hearts were cut into sections and immediately fixed and stored in a 10% neutral buffered formalin solution (Wako, Tokyo, Japan). The tissue slices were then embedded in paraffin and cut into sections. The tissue sections were stained with Gill no. 3 hematoxylin and eosin. The number of polymorphonuclear neutrophils in area at risk was counted using microscopy. Five hearts from each group were examined, and the numbers of polymorphonuclear neutrophils per high power field were counted in five fields using the random observations and the counts were averaged.

2.7. Measurement of myeloperoxidase activity in cardiac tissue

Myeloperoxidase activity was determined in the ischemic cardiac tissue as described previously (Mullane et al., 1985). Briefly, myocardial tissue samples were weighed and homogenized in a potassium phosphate buffer containing 0.5% hexadecyltrimethylammonium bromide (Sigma). The homogenates were centrifuged and then the supernatants were reacted with a 50 mM phosphate buffer (pH 6.0) containing 0.167 mg/ml *o*-dianisidine hydrochloride (Sigma) and 0.0005% hydrogen peroxide. The change in absorbance at 460 nm was measured using the microplate reader (*Ultramark*, BIO-RAD), and the results were expressed as units (U) of myeloperoxidase/100 mg tissue. One unit of myeloperoxidase was defined as that degrading 1 μmol peroxide/min at 25 °C.

2.8. Cell culture

Human umbilical vein endothelial cells were isolated from the normal-term umbilical veins and cultured on 0.1% gelatin-coated tissue culture dishes as described previously (Yoshida et al., 1998) in RPMI-1640 with 20% fetal calf serum (Life Technologies Oriental), endothelial growth factor (25 μg/ml, Funakoshi, Tokyo, Japan), and porcine intestinal heparin (50 μg/ml, Sigma), along with penicillin and streptomycin as antibiotics. HL-60, a maturation-arrested promyelocytic cell line, which has a SLe^x-bearing structure on the surface, was used in this study. The cells have been utilized for the analysis of selectin-dependent leukocyte adhesion in several studies (Ostrovsky et al., 2000; Jeong et al., 2001). HL-60 cells

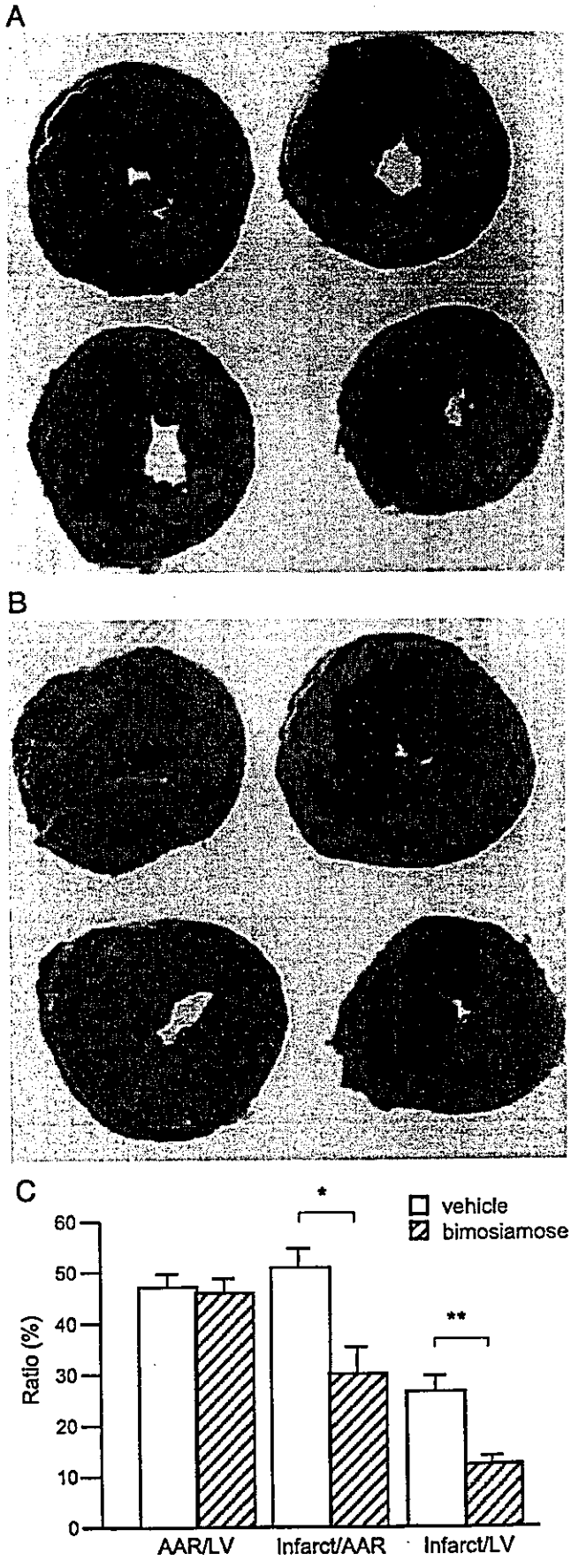

Fig. 2. (A and B) Representative photographs of transverse ventricular sections of the vehicle- and the bimosiamose-treated hearts. Hearts were stained by Evans Blue and triphenyl tetrazolium chloride to confirm the infarct area (white color), the area at risk (AAR) (brick-red color) and the area not at risk (ANAR) (blue color) after 30 min of ischemia and 24 h of reperfusion. (A) Photographs of the vehicle-treated heart. (B) Photographs of the bimosiamose-treated heart. (C) Statistical analyses of infarct size and AAR in hearts from the vehicle- and bimosiamose-treated rats. $^*P=0.01$, $^{**}P<0.01$ compared with rat given vehicle.

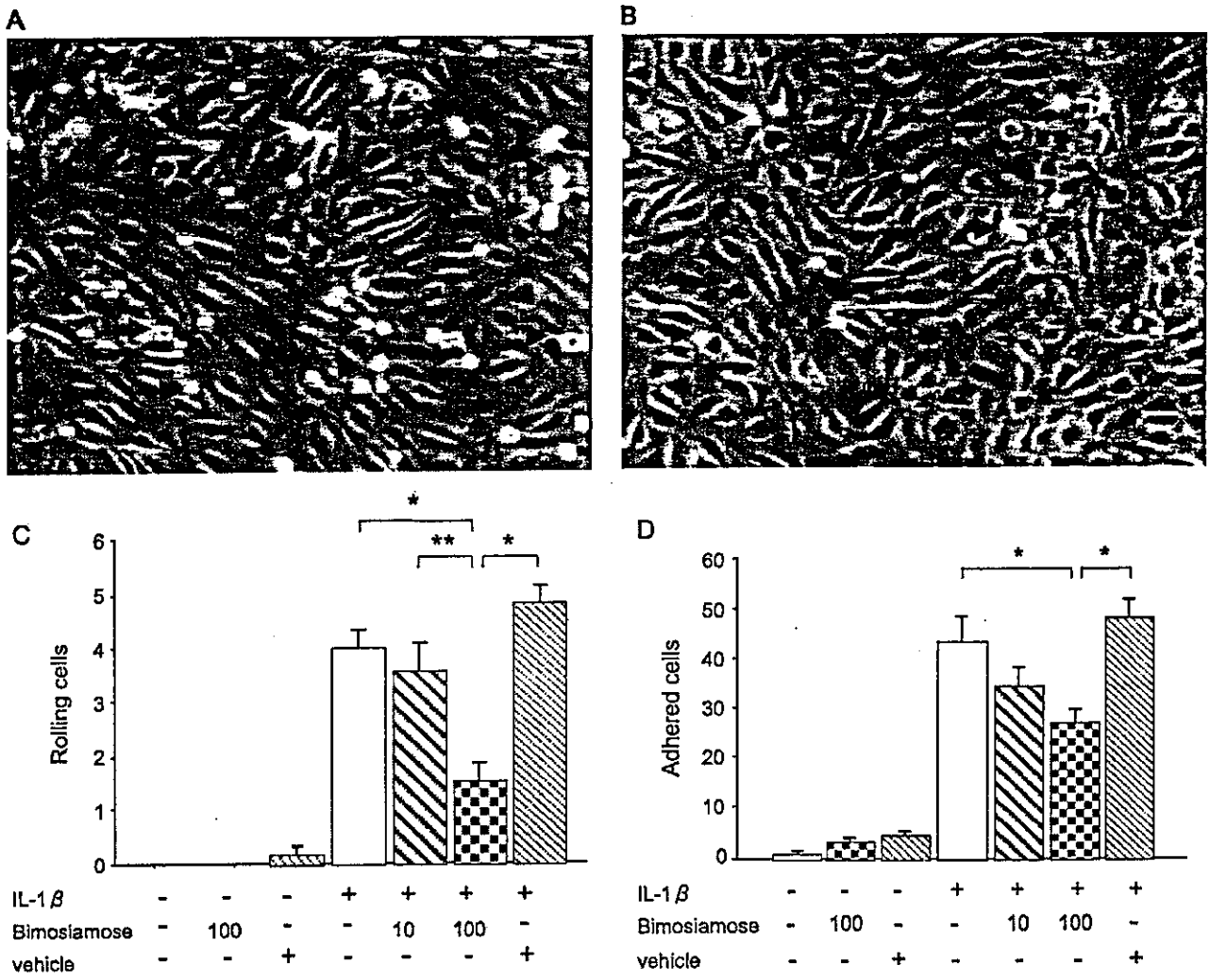

Fig. 5. Efficacy of bimosiamose in neutrophil rolling and adhesion under physiological flow condition. (A and B) Representative photographs of flow plate in condition of HL-60 cells and activated human umbilical vein endothelial cells (Interleukin-1β, 20 U/ml, 4 h) with vehicle pretreatment (100 μM) (A), and with bimosiamose pretreatment (10 or 100 μM) (B). Arrow heads are indicating HL-60 cells adhered to the monolayer of human umbilical vein endothelial cell. (C) Counts of rolling HL-60 cells per high power field under physiological flow condition. $^{*}P<0.001$ compared with non- or vehicle-pretreated human umbilical vein endothelial cells (Interleukin-1β+). $^{**}P<0.02$ compared with bimosiamose (10 μM)-pretreated human umbilical vein endothelial cells (Interleukin-1β+). (D) Counts of adhered HL-60 cells per high power field under physiological flow condition. $^{*}P<0.05$ compared with non- and vehicle-pretreated human umbilical vein endothelial cells (Interleukin-1β+).

effect of bimosiamose in inhibition of cell interaction was observed in a dose-dependent manner.

4. Discussion

Early reperfusion of the ischemic myocardium is the most important strategy for treatment of acute myocardial infarction to salvage the jeopardized myocardium. However, recent studies have revealed that reperfusion evokes a new myocardial damage which is related closely to accumulation of the activated inflammatory cells, especially polymorphonuclear neutrophils (Engler et al., 1983; Neumann et al., 1997; Dreyer et al., 1991). Several adhesion molecules are intervening in attachment of the circulating polymorphonuclear neutrophils to the myocardial vascular endothelium. The most important class of adhesion molecules related to leukocyte rolling, a precursor to firm adhesion and transmigration, is the selectin family. Previous studies have reported that correlation between soluble P- and E-selectin level and the incidence (Shimomura et al., 1998; Suefuji et al., 2000) and the severity (Li et al., 1997) of acute myocardial infarction. Moreover, several studies using animal models have demonstrated that expression of P-selectin (Seko et al., 1996a) and SLe^x (Seko et al., 1996b) is induced by ischemia/reperfusion in myocardium. Furthermore, administration of monoclonal antibody of L-selectin (Ma et al., 1993), P-selectin (Weyrich et al., 1993), E-selectin (Altavilla et al., 1994) and SLe^x (Seko et al., 1996b) and genetic deficiency of P-selectin and E-selectin in mice (Jones et al., 2000) attenuates the myocardial reperfusion injury in vivo.